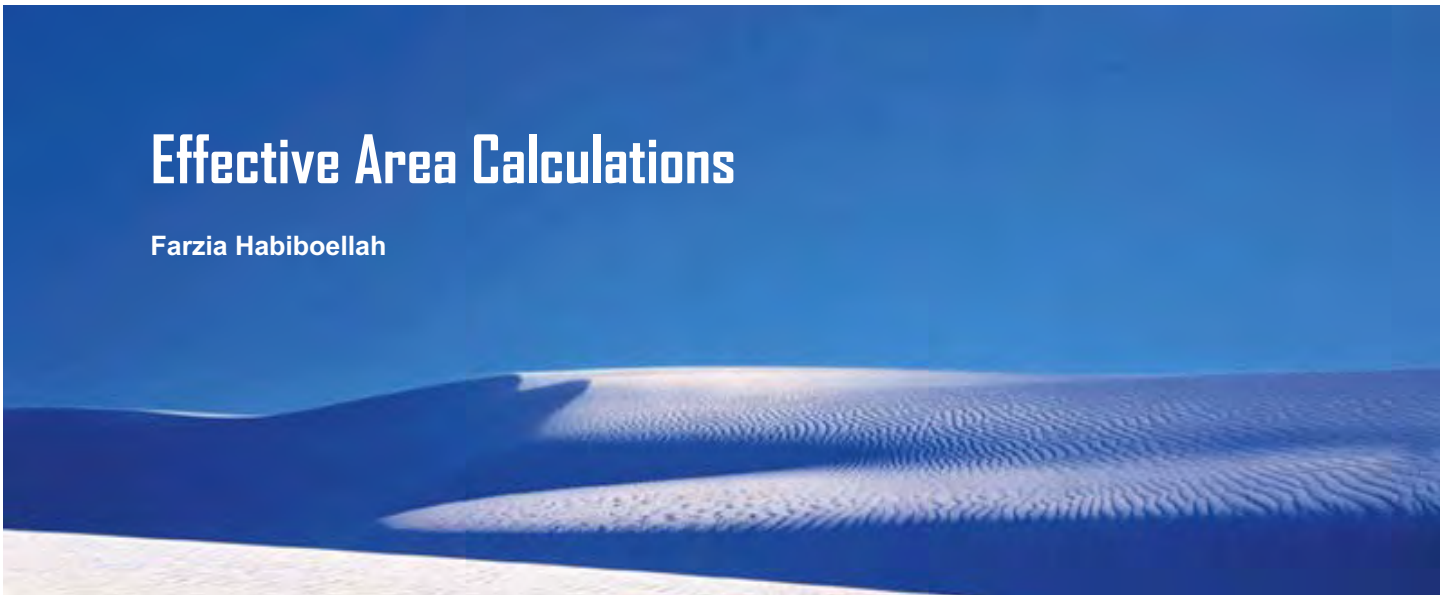


Nederlands Meetinstituut
Department of Mass and Related Quantities
Thijsseweg 11
2629 JA Delft



Effective Area Calculations

Farzia Habiboellah

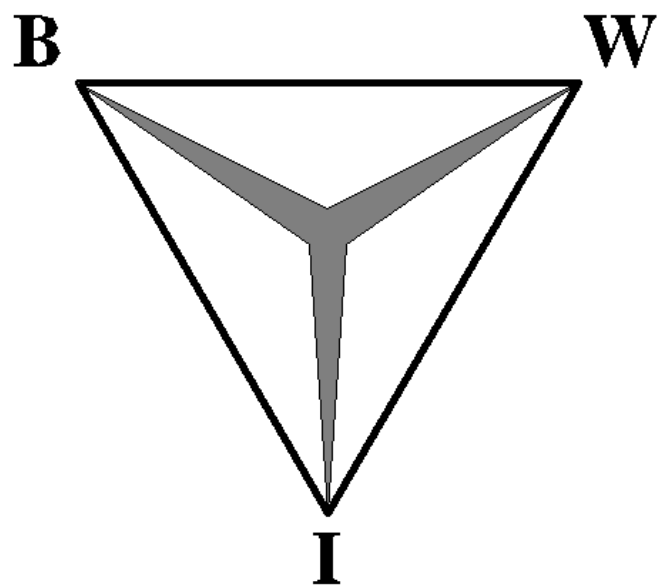


Vrije Universiteit Amsterdam
Faculty of Sciences
De Boelelaan 1081a
1081 HV Amsterdam

vrije Universiteit amsterdam



Effective Area Calculations



Master thesis, October 2007

Vrije Universiteit Amsterdam
Faculty of Sciences
De Boelelaan 1081a
1081 HV Amsterdam

Nederlands Meetinstituut
Department of Mass and Related Quantities
Thijssseweg 11
2629 JA Delft

Effective Area Calculations

Master thesis, October 2007

Preface

As part of the study Business Mathematics and Informatics (BMI) at the *Vrije Universiteit* (VU) in Amsterdam, an external work placement of six months has to be fulfilled. During this work placement theoretical knowledge has to be applied in practice. Special attention has to be paid to the integration of the three fields of expertise, namely Business Administration, Mathematics and Computer Science.

I carried out my internship at the Department of Mass and Related Quantities of the Nederlands Meetinstituut (NMI) in Delft where I performed a study of the calculation method of the effective area of a piston cylinder combination. The past six months have been a valuable experience for me, both on a personal and a content level. Besides a busy and stressful period, it has also been a pleasant and memorable experience.

During my internship I have received support from several people. First and foremost, I would like to thank my internal supervisors at the NMI, Jos Verbeek B.Sc. and Dr. drs. Adriaan van der Veen for their excellent guidance, valuable advice and support during my work placement. A word of thanks also goes to my colleges of the Mass and Relevant Quantities department, especially to Jan Westerhoud and Gerard van Winden, who always had time for a good chat during work time.

Furthermore, I would like to thank my supervisors at the VU, Prof. dr. Jan Bouwe van den Berg (first supervisor) and Prof. dr. G. Jongbloed (second supervisor) for their guidance during my exploration of Pressure Management.

Last but not least, I would like to express my gratitude to my siblings for being there for me at all times, during my education and beyond. I want to thank my parents for their support which gave me the opportunity to continue my study. And I would like to thank my aunt for her excellent care, her listening ear and for giving me a second home in Den Hague during my internship.

Purmerend, June 2007

Farzia Habiboellah

Executive summary

Pressure p is defined as the force of a weight W that is exerted on the surface of a medium (denoted by area A) and can be measured with a pressure balance. The fundamental part of a pressure balance is the piston-cylinder combination (PCC), which consists of a piston that closely fits in a cylinder. To compute the pressure the weight W has to be divided by an area A . In a PCC A refers to the surface of the piston that would be needed to counterbalance the weight W that consists of the weight of the piston and the applied weights.

Due to imperfections in the geometry of the piston and cylinder, there is a small gap between the two components in which a small amount of fluid is pressed upward. This leads to a frictional force F exerted by the fluid to the flanks of the piston that contributes to counterbalancing the weight of the piston, causing it to increase. If the weight increases, the area A also has to increase to maintain the same pressure, causing the piston to behave as if its area is larger than it really is. This larger area is called the effective area or neutral surface of the PCC and is denoted by A_{eff} .

There are two ways of determining the effective area of a PCC: through length measurements and through calibration. Calibration is the process of referring a device that has to be calibrated to a known accurate pressure balance, called a primary pressure balance, so that the deflection of the device can be determined. A requirement for calibration is that the effective area of the primary pressure balance has to be known, which makes it a dependent method. The second one, length measurements, determines the effective area through a function of the measurements and goniometry of both piston and cylinder.

The European organization of national metrology institutes in the EU, came with the idea to compare the effective area calculation methods and its estimated uncertainties of six European National Measurement Institutes (NMIs). Among them was NMI, whose method and results were quite different from the other five institutes and also has a higher uncertainty. Another finding was that four out of the six participating NMIs basically used the same method. This method is described in based on Dadson's theory. That is why the Mass and Related Quantities department of the NMI would like to implement a new measurement method that leads to a better estimate of the effective area with considerable lower uncertainties. The objective of this work has been described as:

'Studying Dadson's theory and the method used by the NMI to determine which method should be used to calculate the effective area in order to obtain a more accurate estimate and develop the corresponding uncertainty model'

In modeling assumptions have to be made to simplify a problem so that it is possible to have it modeled while it is still comprehensible. The trick is to find a balance between keeping the model comprehensible without losing its connection to reality. The model that is used by NMI is based on the assumptions that the piston and cylinder are perfectly straight and straight and thereby assumes that there is no extra frictional component F . The radius of the effective area can therefore be computed by taking the average value of the piston and cylinder radius. In reality both piston and cylinder are not perfectly round or straight, which leads to deviations in the input parameters of the model and thereby in its output.

The main differences between the NMI model and the model based on Dadson's theory is that Dadson does not assume that the piston and cylinder are perfectly straight. In Dadson's model this results in the piston and cylinder radii being dependent of an index that represents the height of the measured point and thereby reckons with the imperfections in the PCC. In the NMI model one radius is calculated that is the average of the piston and cylinder radius.

The proposed model is based on Dadson's theory. In the corresponding uncertainty model the straightness component is dropped, because straightness is not assumed anymore. Added to the model is uncertainty due to the use of the Trapezium Rule that is used to approximate the integrals in Dadson's formula. In both models it is assumed that the length measurements are independent of each other when according to the SWI this is not true. In Appendix B an uncertainty model is developed through the use of uncertainty propagation under the assumption that the measurements are dependent.

Both models were implemented in C and the results were compared with the results of the PTB, the NMI of Germany, which are in line with those of the SMU, LNE and IMGIC. In contrast to the results of NMI the results of the proposed model correspond to those of the PTB model. Therefore it can be concluded that not only is the proposed model a good application of Dadson's theory, but the proposed model is also more credible than the current NMI model.

Contents

Preface	4
Executive summary	5
Contents	7
Symbols	9
Chapter 1 Introduction	12
1.1 Nederlands Meetinstituut.....	12
1.2 Background.....	12
1.3 Objective and Scope	13
1.4 Structure of the thesis	14
Chapter 2 Pressure measurement	16
2.1 Introduction	16
2.2 The effective area of a PCC.....	16
2.3 Measurement uncertainty	18
2.4 Calibration	20
2.4.1 The Pressure-generate Method	20
2.4.2 The p-method.....	21
2.4.3 Effective Area Determination.....	21
Chapter 3 Length Measurements.....	23
3.1 Introduction	23
3.2 Length, roundness and straightness	23
3.3 The mathematical model	25
3.4 Uncertainties.....	27
3.4.1 Straightness.....	27
3.4.2 Roundness.....	28
3.4.3 Diameter measurements	28
3.4.4 Uncertainty of the effective area computation	29
3.5 Application on NMI dataset.....	30
3.5.1 Effective area calculation	30
3.5.2 Uncertainty calculation.....	30
Chapter 4 Dadson's theory	32
4.1 Introduction	32
4.2 The effective area of a ideal PCC.....	32
4.2.1 The virtual piston model.....	33
4.2.2 Location of the neutral surface	34
4.3 The effective area for a simple PCC.....	35

Chapter 5	Proposed model	38
5.1	Introduction	38
5.2	Perfectly straight or not?.....	38
5.3	The trapezium rule.....	39
5.4	Uncertainty	40
5.4.1	Uncertainties due to numerical procedures	41
5.4.2	Systematic and random errors affecting the uncertainty	42
Chapter 6	Results	45
6.1	Introduction	45
6.2	Datasets.....	45
6.3	Effective area calculations.....	45
Conclusion	48
Appendix A	NMi Measurement	50
A.1	The measurement model for the diameter	51
Appendix B	Uncertainty model.....	52
B.1	Uncertainty propagation.....	52
B.2	Example	53
B.3	Propagation Model.....	54
References	57

Symbols

A	Effective area	m^2
A_0	Effective area at pressure $p = 0$ Pa	m^2
$A_{0,20}$	Effective area at pressure $p = 0$ Pa en reference temperature $t = 20$ °C	m^2
F	Force	N
g	Gravitational acceleration or gravity	N/kg
h	Space between piston and cylinder	m
h_0	Space between piston and cylinder at height $x = 0$	m
k	Coverage factor-	
m	Mass	kg
p	Pressure	Pa
p_0	Initial value of reference pressure	Pa
r	Distance to the outside of the piston	m
r_0	Distance to the outside of the piston at height $x = 0$	m
r^*	Distance to the neutral surface	m
r_0^*	Distance to the neutral surface at height $x = 0$	m
R	Distance to the inside of the cylinder	m
R_0	Distance to the inside of the cylinder at height $x = 0$	m
t	Temperature	°C
u	Shape deviation of the piston	m
u^*	Combined shape deviation of the piston and cylinder	m
U	Shape deviation of the cylinder	m
W	Weight of applied masses incl. the mass of the piston	N
w	Weight of the annular cross-section between the piston- and neutral surface	N
W'	Downward gravitational force on W	N
w'	Downward gravitational force on w	N
z	Height level of the piston en cylinder	m
α	Thermal expansions coefficient	K^{-1}
ε	Small value defined as $1 + \frac{h}{r}$	
λ	Elastic deforming coefficient	Pa^{-1}
ρ	Density	kg/m^3
ρ_{amb}	Air density	kg/m^3
ρ_m	Density of the weights and piston	kg/m^3
Π	External pressure at level x	Pa

Acronyms:

PCC	Piston-cylinder combination
NMi	Nederlands Meetinstituut
NMI	National Metrological Institute
EUROMET	European organization of national metrology institutes
SWI	Studiegroep Wiskunde met de Industrie

Chapter 1 Introduction

1.1 Nederlands Meetinstituut

During my internship I worked at the Mass and Related Quantities Department of the NMI (“Nederlands Meetinstituut”). NMI maintains the Dutch measurement standards and develops new measurement standards and reference materials. NMI is a full subsidiary of Holland Metrology N.V., which in turn is owned by TNO. The institute was established after the privatization of the former Dutch Legal Metrology Service (*Dienst van het IJkwezen*) on the 1st of May 1989. As of 21 February 2001, the company became part of the Dutch Organization for Applied Scientific Research TNO. NMI B.V. is the holding company of three subsidiaries: NMI Van Swinden Laboratorium B.V., NMI Certin B.V., and Verispect B.V. NMI van Swinden Laboratory B.V. is the Dutch national standard institute.

Mass and Related Quantities is a department of NMI van Swinden Laboratorium and is responsible for the maintenance and development of measurement standards for mass, pressure, force and viscosity measurements. My internship assignment concerned the field of pressure measurement. Pressure is realized using weights and pressure balances. They use their own accurate pressure balance to calibrate the pressure balances of clients. The pressure balance consists of a piston-cylinder combination of which the surface needs to be accurately determined.

1.2 Background

The pressure p is defined as the magnitude of a force F that is exerted on the surface of a medium denoted by area A (force per unit area). This leads to the following equation:

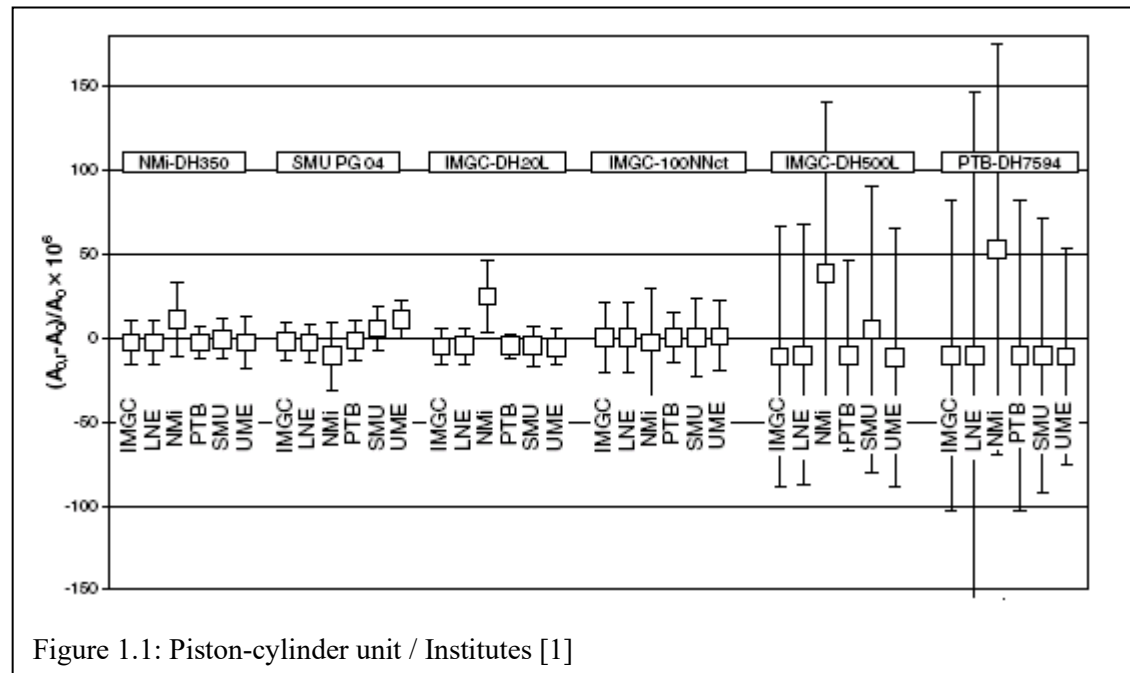
$$p = \frac{F}{A} \tag{1}$$

In a piston-cylinder combination (PCC) A refers to the surface of the piston that would be needed in an ideal situation to counterbalance the weight W of the piston just from the pressure force F . The problem is that A can differ from the actual surface of the piston, which can lead to inaccurate pressure measurements. Due to irregularities of the PCC and other effects the piston behaves as if its area were slightly larger than it actually is. This area is referred to as the effective area and is denoted by A_{eff} .

The question remains how to calculate this slightly larger area. National Measurement Institutes (NMIs) all over the world struggle with this problem. EUROMET, the organization of NMIs in

Western Europe, came up with the idea to compare the effective area calculation methods and the estimated uncertainties of six European NMIs. This comparison was carried out as EUROMET Project 740 [1].

Six sets of measurement data were run through the models of each of the six participating institutes. The zero line (Figure 1.1) is the average of the results of the six institutes. The distance from the zero line to the squares represents the deviation of one institute from the average.



The bars on both sides of the squares indicate the standard uncertainty $u(A_0)/A_0$ obtained by each institute. Among them was NMI, whose method and results were quite different from the other five institutes.

1.3 Objective and Scope

In comparison with the methods of other European institutes, the method used by NMI to calculate the effective area is quite simple. NMI calculates the effective area by using average values of the piston and cylinder radii at different heights. Figure 1.1 shows that this approach leads to different results and a higher uncertainty in comparison with the other institutions. In a review of the methods used in EUROMET Project 740, it was concluded that four out of six NMIs basically used the same method [2]. This method is described in [3] and in this work this method will be referred to as Dadson's theory.

Given the importance of accurate measurements, the demand for accurate measurement methods has increased. That is why the Mass and Related Quantities department of the NMI would like to implement a new calculation method that leads to a better estimate of the effective area.

"Better" should be understood in terms of a smaller bias as well as lower uncertainties. The objective of this work can therefore be defined as:

'Studying Dadson's theory and the method used by the NMI to determine which method should be used to calculate the effective area in order to obtain a more accurate estimate and develop the corresponding uncertainty model'

The following questions can be derived from the aforementioned objective:

- What is a pressure balance and what has its structure to do with the determination of the effective area?
- What is uncertainty and why does it play such an important role in the recommendation of a model?
- How is Dadson's theory constructed and to what extent does it differ from the current method used by the NMI?

1.4 Structure of the thesis

In chapter 2 the first question will be covered. Besides definitions for pressure, pressure balances and calibration, the main processes in pressure measurement will be discussed. It is necessary to cover these subjects to obtain a better understanding of the main subject: the effective area. Furthermore, the concepts of measurement uncertainty and metrological traceability are briefly introduced.

In chapter 3 length measurements and the currently used method of the NMI will be discussed. This method calculates the effective area as the average of all the dimensional data to determine the neutral surface as an average of the piston and cylinder radius.

After going through the current NMI model, Dadson's theory will be covered in chapter 4. Four out of the six models used by the National Measurement Institutes participating in EUROMET Project 740 are based on this theory.

Now that the basic principles of both types of models have been outlined, they can be compared to each other. Considering the strengths and weaknesses of both types of models, a new model will be recommended and implemented. The modeling work is covered in chapter 5 and the results obtained with the new model in chapter 6.

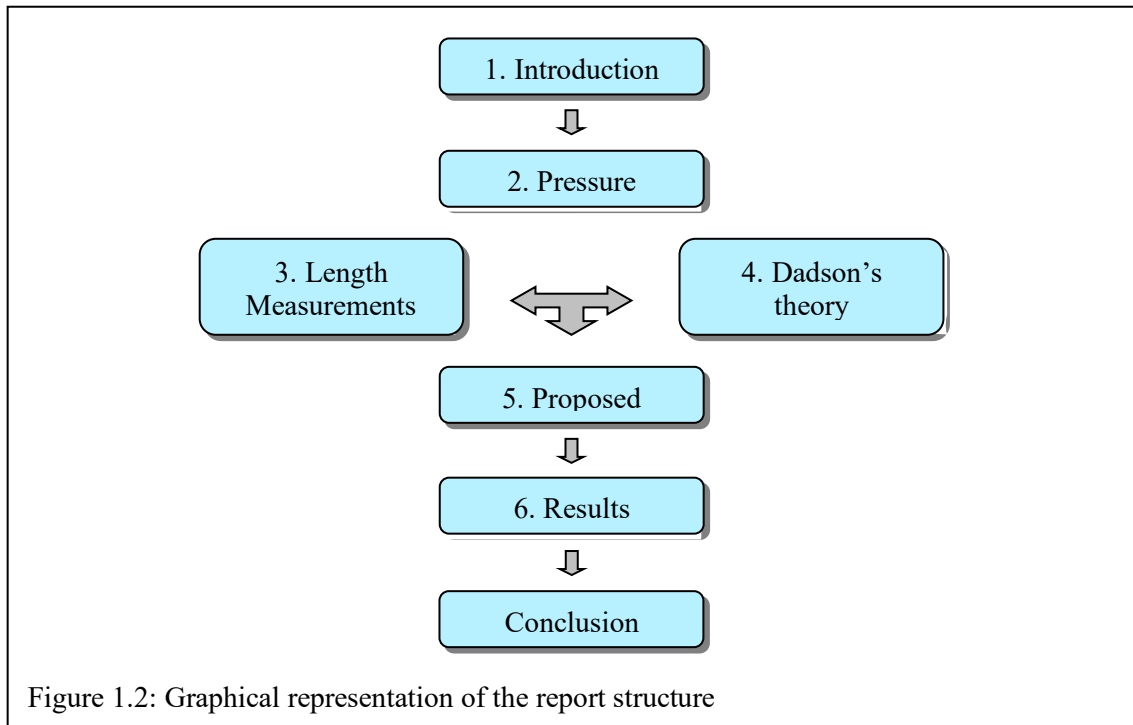


Figure 1.2: Graphical representation of the report structure

Chapter 2 Pressure measurement

2.1 Introduction

The Mass and Related Quantities Department of NMI is active in pressure measurement and in the calibration, testing and certification of pressure balances. This chapter starts with explaining the basic structure of a pressure balance and gives a detailed description of the piston-cylinder combination (PCC), which is part of a pressure balance, and its relevance to the effective area. The last two sections will cover calibration and uncertainty and their importance for accurate estimation of the effective area.

2.2 The effective area of a PCC

The pressure balance (see Figure 2.1), also referred to as "deadweight tester" or "pressure gauge", is an instrument that instantly measures the pressure in terms of force and mass. The Britannica Concise encyclopedia [4] gives the following definition for pressure:

“Pressure is a perpendicular force per unit area, or stress at a point within a confined fluid. A solid object exerts pressure on a floor equal to its weight divided by the area of contact.”

Thus the pressure is determined by dividing the weight W of the downward gravitational force due to the applied masses by an area A and can be represented by the following equation:

$$p = \frac{W}{A} \quad (2)$$

p = pressure [Pa]

W = weight [N]

A = area [m^2]

Sometimes the weight W in equation (2) is denoted by the force F , but we will use the symbol W because later on in this report we will introduce a frictional component that will be denoted by F . The weight can be expressed as a mass m on which a gravitational force g works. This leads to the following equation:

$$W = m \cdot g \quad (3)$$

m = mass [kg]

g = gravitational constant [N/kg]

The main components of a pressure balance are the manometer from which one can read the pressure, the tube system that contains a fluid¹ on which the pressure will be exerted and the piston-cylinder combination. By turning the screw the amount of fluid that is pressed into the reservoir by the weight W on the piston is determined. It works by loading the piston (of cross sectional area A), with the amount of weight (W) that corresponds to the desired pressure that is calculated according to equation (2). Note that the weight W includes the weight of the piston. The piston then pressurizes the whole system by pressing more fluid into the tube system, until the dead weight lifts off its support.

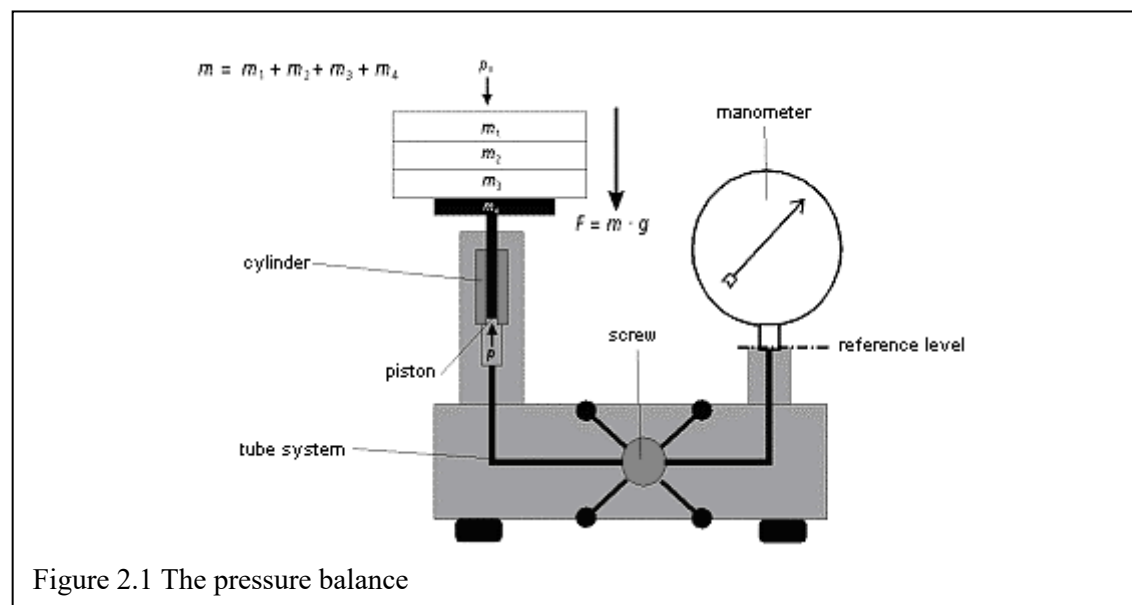


Figure 2.1 The pressure balance

When a measurement is carried out, a mass will be placed on the piston that is spinning in the closefitting cylinder (see Figure 2.1), this is done to keep the friction between them as small as possible. The absolute pressure is then given by:

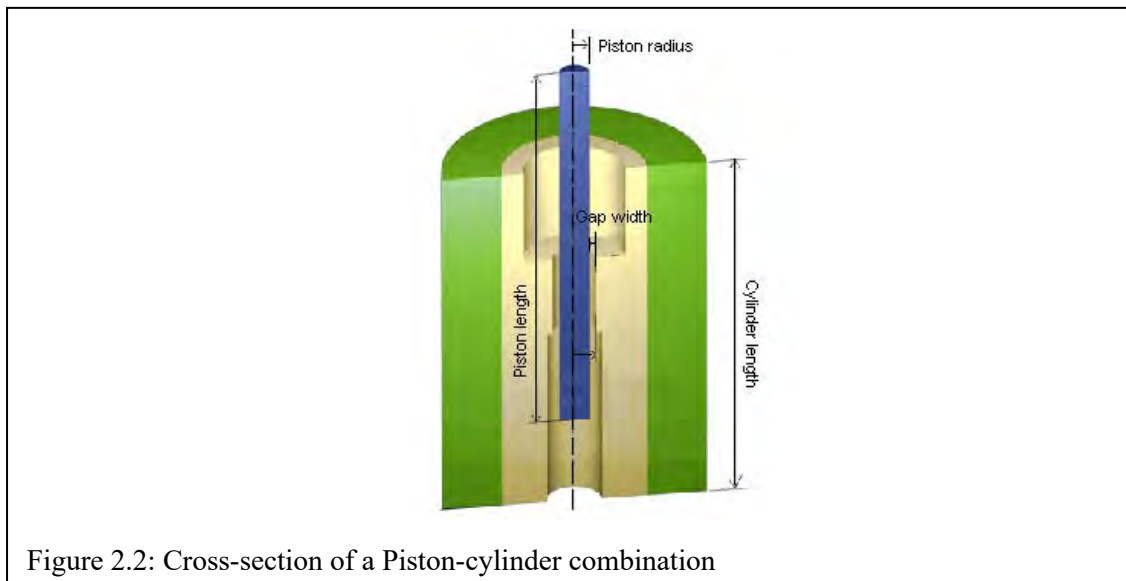
$$p = p_2 + \frac{(m \cdot g)}{A} \quad (4)$$

- p_2 = pressure on top of the piston [Pa]
- m = mass [kg]
- g = gravity [N/kg]
- A = area [m²]

The equilibrium of the piston cylinder combination is achieved when the piston and the mass pieces placed above descent in a constant manner. The rate of descent of a piston is dependent on the pressure, temperature and the goniometry of the piston cylinder combination.

¹ Gas, vapour or liquid

In Figure 2.2 a cross section of a PCC is shown. In the center of the PCC there is a constriction in the cylinder to keep the fluid in the tube system from leaking into the space above the constriction. But this constriction should not be too tight, because the piston still has to be able to spin in the cylinder, which requires a small gap between the piston and cylinder. With the naked eye, the surface of the piston and cylinder in the gap seem perfectly straight, but on a microscopic level this is not the case. In the gap a small amount of fluid is pressed upwards, which leads, in combination with the imperfections in the PCC, to a frictional force exerted by the fluid to the flanks of the piston. This force F contributes to counterbalancing the weight of the piston:



Because of this frictional force F that is exerted on the flanks of the piston, the weight W effectively increases. In chapter three we will go deeper into the mathematical aspect of the weight increase. Through equation (2) it can be seen that if the weight increases, the area A also has to increase to maintain the same pressure. Thus the force F causes the piston to behave as if its area is larger than it in reality is. This larger area is called the *effective area* of the PCC and is denoted by A_{eff} . In chapters 3 and 4 two models will be discussed that use different calculation methods to provide an estimate for the effective area.

2.3 Measurement uncertainty

No measurement is perfect. If a measurement is repeated several times, a distribution of results will be obtained. The dispersion in these results can be described in terms of uncertainty of measurement. Measurement instruments, measurement standards, environmental factors, among others, contribute to the overall uncertainty of measurement [5]. Depending on the model defining the quantity to be measured (*measurand*) [5] and the uncertainty associated with each of these factors, some influencing factors contribute more than others to the overall uncertainty.

The mathematical model of the measurand of a pressure balance is given by [6]:

$$p_s = \frac{m_s \cdot 0.99985 \cdot g_l}{A_s \cdot (1 + \alpha \cdot (t_{pcu} - 20^\circ \text{C}))} \quad (5)$$

m_s	=	Mass
A_s	=	Effective area of the PCC
g_l	=	Gravitational acceleration or gravity
α	=	Temperature coefficient
t_{pcu}	=	Temperature of the PCC

In this equation, the factor 0.99985 comes from the buoyancy correction of weightweights with known masses. This correction corresponds to the exerted upward force as a result of the amount of displaced air of which the volume is equal to the volume of the weightweights and is calculated by $(1 - \rho_{\text{amb}} / \rho_m)$ [6], where ρ_{amb} denotes the air density (1.2 kg/m^3) and ρ_m the density of the weights (8000 kg/m^3):

$$1 - \frac{1.2 \text{ kg/m}^3}{8000 \text{ kg/m}^3} = 0.99985 \quad (6)$$

Every variable in equation (5) contributes to the uncertainty of a pressure measurement. Such a model is often explicit, that is, of the form

$$p_s = f(m_s, A_s, g_l, \alpha, t_{pcu})$$

For convenience we rename the input quantities m_s, A_s, g_l, α and t_{pcu} to x_1, x_2, x_3, x_4 and x_5 . If the uncertainty associated with the input quantities x_i are known, the uncertainty associated with y (p_s) can be expressed as follows using the uncertainty propagation formula,

$$u^2(y) = \sum_i c_i^2 u^2(x_i) + \sum_{i=1}^{n-1} \sum_{j=i+1}^n c_i c_j u(x_i, x_j) \quad (7)$$

where c_i denotes the sensitivity coefficient. The sensitivity coefficient is the partial derivative of the measurement model f with respect to one of the input quantities x_i . It expresses the sensitivity of the uncertainty in y for the uncertainty in x_i .

The uncertainty propagation formula can be written in matrix form as follows [4]:

$$u^2(y) = \mathbf{c} V_x \mathbf{c}^T, \quad (8)$$

where \mathbf{c}^T denotes the transpose of the row vector \mathbf{c} and V_x denotes the uncertainty matrix of the input variables.

In Table 2.1 the columns show the input variables (x_i [x_i]), the estimate (value), the uncertainty associated with the measured values ($U(x_i)$), the standard uncertainty ($u(x_i)$), the contribution factor (partial derivative c_i) and the uncertainty contribution ($c_i u(x_i)$). By taking the partial

derivative of every influence factor its uncertainty contribution can be computed. In the last column of Table 2.1 it can be seen that the effective area has the largest uncertainty contribution in the uncertainty of a pressure measurement.

x_i [x_i]	Value	$U(x_i)$	$u(x_i)$	c_i	$c_i u(x_i)$
m_s [kg]	10.000 42	0.000 01	0.000 005	10000	0.05
A_s [m ²]	9.804 854 10^{-4}	0.000 29 10^{-4}	0.000 15 10^{-4}	1.0 10^8	1.53
g_l [N/kg]	9.812 42	0.000 02	0.000 01	10 204	0.10
α [1/°C]	1.10^{-5}	0.1 10^{-5}	0.05 10^{-5}	130000	0.07
t_{pcu} [°t]	21.3	0.2	0.1	1	0.10

Table 2.1 Uncertainty contributions

2.4 Calibration

Calibration is the process of referring a device that has to be calibrated to a known accurate pressure balance, called a primer pressure balance, so that the deflection of the device can be determined.

There are three generally known methods to calibrate a deadweight tester:

- pressure generate-method,
- p-method and
- most fundamental method where the effective area of a PCC is determined.

With each method so called “cross-float”-measurements are carried out. During these cross-float measurements two pressure balances are connected and balanced out by tuning both balances so that they will generate precisely the same pressure (see Figure 2.3). If both PCCs are in balance with each other, it holds that the pressure p_R generated by the referential combination and the pressure p_X are equal. Usually the accuracy of a primary pressure balance is at least four times greater than the equipment being calibrated.

2.4.1 The Pressure-generate Method

The *pressure-generate* method calibrates an unknown pressure balance by determining if the pressure that is generated by standard weights resembles the pressure that is mentioned on the weights. For every measure point a “cross-float”-measurement must be executed with the unknown and primary pressure balance. According to the measurement results it can be determined if the pressure balance meets its specifications.

An advantage of this method is that the calculations are relatively simple. There is no need to deal with different kinds of corrections. The drawback of this method is the fact that the

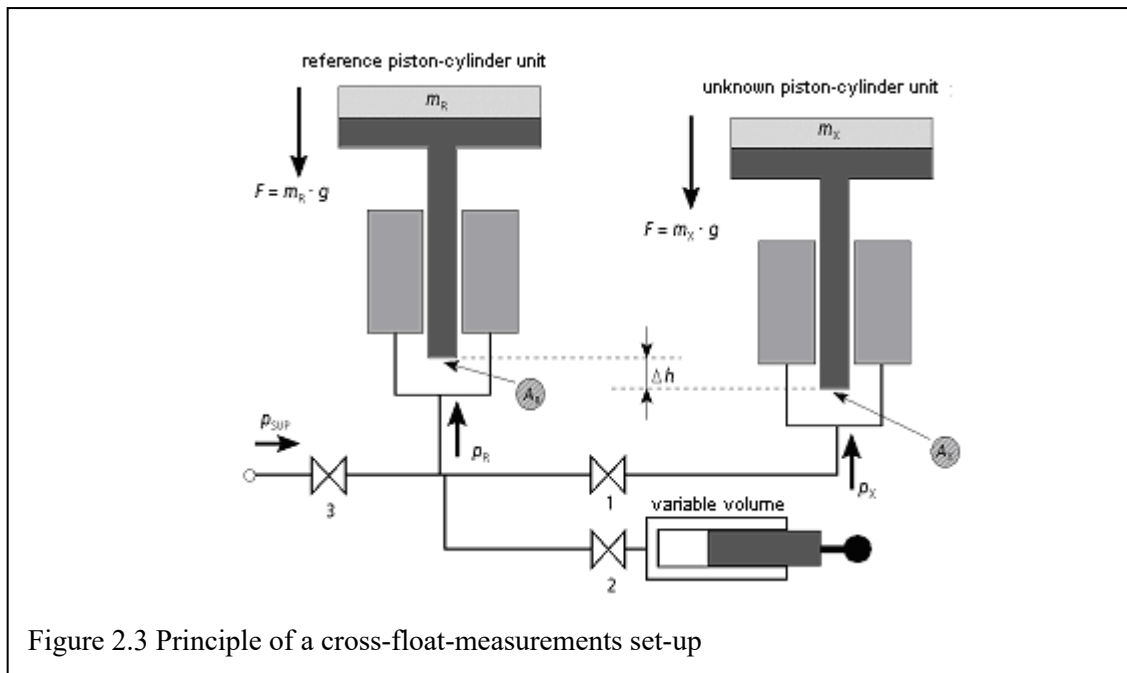


Figure 2.3 Principle of a cross-float-measurements set-up

pressure balance is calibrated on a fixed number of points where the combination of the weights is also fixed. This means that the calibration is only valid if the same combinations of the weights are used.

2.4.2 The p-method

The *p-method* determines the sensitivity and the starting pressure of the reference pressure balance. The sensitivity of a PCC expresses the pressure (kPa) that is generated per kilogram mass and therefore has the unit kPa/kg. The sensitivity of a PCC is immediately calculated from the observations without knowledge of the starting mass and the location of the bottom of the piston in floating condition. The starting mass is the mass of the piston. For every measured point *i* the pressure on the reference level is calculated. This is done because the reference levels of the referential and primary pressure balance are equal to each other: $p_R = p_X$. On every measure point the sum of the mass of the used weights excluding the mass of the piston on the pressure balance are known. If the sensitivity is accurately known, the pressure that is generated by the piston, which is called the starting pressure, can be calculated.

The advantage of this method is that the PCC does not have to be disassembled and that several corrections like the difference in the reference levels are included in the sensitivity. In contrast to the “pressure generate”-method the mass of the weights have to be determined. The drawback of this method is that the uncertainty in the calculated start value of the starting pressure is relatively high.

2.4.3 Effective Area Determination

The third method is based on the determination of the effective area, the mass of the accompanying weights and the mass of the piston. Furthermore the reference level of the

pressure balance is calculated according to the goniometry of the piston. In a balanced situation of two pressure balances R and X the following equation holds:

$$p_R = p_X \rightarrow (m_R \cdot g)/A_R = (m_X \cdot g)/A_X \rightarrow m_R/A_R = m_X/A_X \quad (9)$$

Where p stands for pressure, m for mass and A for the effective area. The advantage of this method is that the pressure balance is fully characterized and that the results are obtained with the smallest possible uncertainty. On the other hand the calculations, measurements and the determination of correction factors are rather complex.

Chapter 3 Length Measurements

3.1 Introduction

After introducing the concept *effective area* in section 2.2, now its computation can be addressed. There are two ways of determining the effective area of a PCC.

The first method, calibration, was covered in the last section of chapter 2. A requirement for calibration is that the effective area of the primer pressure balance has to be known, which makes it a dependent method.

The second and independent method is from geometric measurements. The area on which the applied pressure is generated is no longer the area of the cross section of the piston, but a function of the measurements and geometry of both piston and cylinder. This chapter deals with the geometric measurements and how these are used to calculate the effective area of a PCC. The uncertainty of this method will be covered in section 3.4.

3.2 Length, roundness and straightness

The basic assumption when characterizing a PCC is that both cylinder and piston are cylindrical. In the mathematical sense, this means that, e.g.,

each cross-section is a circle with a constant radius

the principal axes of the cylinder and piston coincide and can be represented by a straight line

To compute the effective area, information about the geometry of the PCC is needed. To obtain values of the length measurements of the piston and cylinder, the PCC is measured by the Length Department of NMI at several levels on the vertical axis. At every level the diameter is measured more than once. The diameter at level l is determined by taking the average of those measurements. In Table 3.1 the radius values for a PCC are given, which are calculated by dividing the average diameter by two.

Height (l) mm	Piston (r) mm	Cylinder (R) mm	r-R mm
0,0	17,66634	17,66786	0,00153
0,4	17,66634	17,66782	0,00148
1,5	17,66634	17,66781	0,00147
5,5	17,66636	17,66720	0,00084
10,5	17,66634	17,66703	0,00068
15,5	17,66634	17,66697	0,00063
20,5	17,66633	17,66694	0,00061
25,5	17,66632	17,66698	0,00066
30,5	17,66632	17,66701	0,00069
35,5	17,66631	17,66712	0,00080
39,0	17,66632	17,66751	0,00119
39,6	17,66632	17,66743	0,00111
40,0	17,66632	17,66745	0,00113

Table 3.1: Average radius of the PCC at height h [7]

When a set of numbers is extended with values that lie *outside* the range of the measured values, it is called extrapolation. When a set of numbers is extended with values that lie *within* the range of the measured values it is called interpolation. In Table 3.1 the diameters of the piston and cylinder on the top and the bottom of the narrowing are specified by gray numbers and are acquired by extrapolation. The reason for this lies in the fact that at the top and bottom shape deviations occur, which obstructs accurate measurement of the diameter at these heights. At every height, except those of which the radius values are obtained by extrapolation, the diameter is measured several times. The diameter values in Table 3.1 are average values.

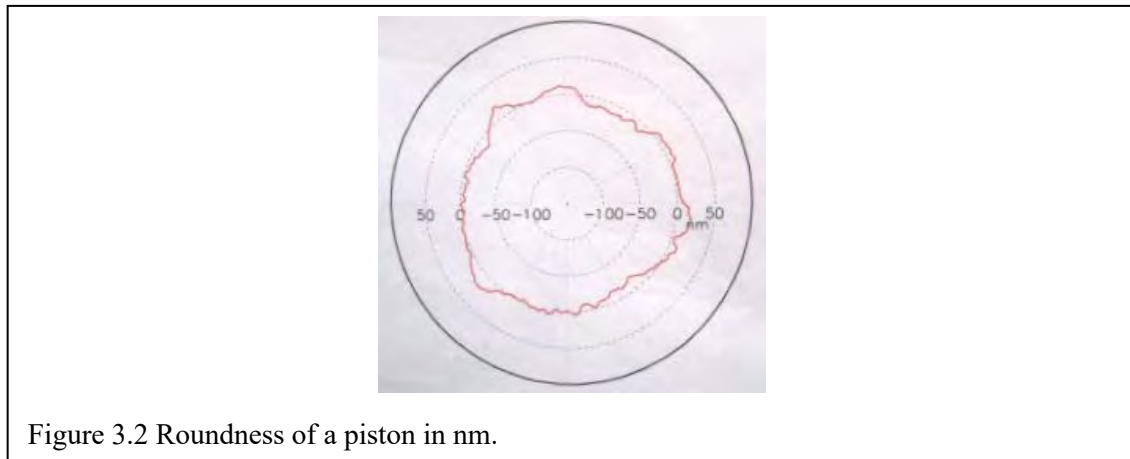
(h) mm Height	Roundness (mm)		Straightness (mm)	
	Piston	Cylinder	Piston	Cylinder
0.0	no data	no data	0.00001	0.00055
0.4	no data	no data	0.00001	0.00050
1.5	0.000143	0.000058	0.00001	0.00049
5.5	0.000137	0.000049	0.00003	-0.00012
10.5	0.000114	0.000068	0.00001	-0.00029
15.5	0.000084	0.000040	0.00001	-0.00035
20.5	0.000063	0.000044	0.00000	-0.00038
25.5	0.000082	0.000042	-0.00001	-0.00034
30.5	0.000079	0.000043	-0.00001	-0.00031
35.5	0.000126	0.000064	-0.00002	-0.00020
39.0	0.000151	0.000055	-0.00001	0.00019
39.6	no data	no data	-0.00001	0.00012
40.0	no data	no data	-0.00001	0.00014

Table 3.2 Roundness and straightness deviation [7]

In Table 3.2 the roundness and straightness deviations on height h are given. The piston and cylinder have a nominal radius, but in reality both piston and cylinder are not perfectly round, which leads to deviations in the roundness. The Length Department has equipment that

measures the deviation between the nominal radius and the true radius of the circle on height h . At every height the maximum deviation is computed and represented in Table 3.2.

The straightness deviations in Table 3.2 are not measurements, but are computed by subtracting the radii values of the piston and cylinder series (see Table 3.1) by its mean. In Figure 3.2 a schematic drawing of the cross-section of a piston is shown (red line).



3.3 The mathematical model

The model used by NMI is rather simple in comparison to the models used by the other participants of the EUROMET project 740 and is based on the following assumptions for both piston and cylinder:

- The midpoint is the same on every height
- They share the same midpoint.
- They are perfectly round at every height.
- They are perfectly straight at every height.

The first two assumptions are crucial, because developing a model will become quite complicated without them. The second assumption deals with the fact that the piston may move within the cylinder while it is spinning.

If the assumption were made that both piston and cylinder are perfectly round, it would hold that the piston and cylinder would have a radius on every height that fits the cross-section perfectly. If then the assumption were made that both piston and cylinder are perfectly straight, it would mean that their radius is the same on every height. The radius of the piston and cylinder on level i will be denoted by respectively r_i and R_i , where n stands for the number of measurement points.

$r = (r_1, \dots, r_n)$ The piston radii of point i , where $i = 1, \dots, n$.

$R = (R_1, \dots, R_n)$ The cylinder radii of point i , where $i = 1, \dots, n$.

The radius for the effective area r^* is computed by taking the average of the average piston and cylinder radii. This can be modeled as:

$$A_{eff} = \pi(r^*)^2, \text{ with } r^* = \left(\frac{\bar{r} + \bar{R}}{2} \right) \quad (10)$$

\bar{r} The average of the piston radii
 \bar{R} The average of the cylinder radii

From the second assumption, it can be derived that the surfaces of the piston and cylinder are perfectly straight and for that reason no friction component has to be modeled. But the assumptions that lead to the biggest simplification of the ‘real world’ into the model are “*the midpoint is the same on every height*” and “*they share the same midpoint*”. In reality the midpoints do not necessarily lie on the vertical axis of both piston and cylinder. In fact they can be shaped as a corkscrew. The last assumption which states that the piston and the cylinder share the same midpoint has to be made because in reality the piston rotates within the cylinder and could therefore change position, which will lead to a shift of midpoint of the piston.

3.4 Uncertainties

The goal of the modeling is to develop a model that describes reality as close as possible. In many cases this leads to very complex models and more often it happens that it is not possible to build a model that is a 100% replica of real situation. That is why assumptions have to be made that simplify the problem so that it is possible to have it modeled and still comprehensible. The consequence of assumptions and the occurrence of imperfections during the length measurements will lead to an uncertainty of the models input and thereby of the models output.

According to the NMI method the uncertainty of their models output, the effective area, consists of two main components: shape deviations and length measurements [7]. The first component is a result of the assumptions that are made in the mathematical model, namely that the piston and cylinder are perfectly straight and round. The uncertainty due to these assumptions can be expressed in the shape deviation parameters $u^2(s)$ and respectively $u^2(t)$. The error that is made during the measure process of the radii expressed in the length measurement parameter $u^2(l)$.

3.4.1 Straightness

The uncertainty caused by shape deviations in the piston and cylinder $u(s)$ can be split in $u(s_r)$ (piston) and $u(s_R)$ (cylinder). The radius data in Table 3.1 are assumed to be normally distributed and consist of 15 points. If that is the case, the standard deviation of the piston and cylinder radii can be defined as:

$$\sigma_r = \sqrt{\frac{1}{n-1} \sum_{i=1}^n (r_i - \bar{r})^2} \quad (11)$$

and likewise,

$$\sigma_R = \sqrt{\frac{1}{n-1} \sum_{i=1}^n (R_i - \bar{R})^2} \quad (12)$$

Assuming mutual independence of the r_i and R_i respectively, the standard uncertainties associated with \bar{r} and \bar{R} can be determined by dividing the standard deviations of the piston and cylinder radius by the square root of the number of measured points:

$$u(s_r) = \frac{\sigma_r}{\sqrt{n}} \quad (13)$$

and likewise,

$$u(s_R) = \frac{\sigma_R}{\sqrt{n}} \quad (14)$$

The combined standard uncertainty $u(s)$ can be computed by taking the square root of the sum of squares of $u(s_r)$ and $u(s_R)$:

$$u(s) = \sqrt{u(s_r)^2 + u(s_R)^2} \quad (15)$$

3.4.2 Roundness

The uncertainty caused by deviations in the roundness of the piston and cylinder will be denoted by $u(t_r)$ and roundness $u(t_R)$. They are calculated by dividing the maximum roundness deviation of Table 3.2 by $2\sqrt{3}$ because the roundness deviations are assumed to be Rectangular distributed.

$$u(t_r) = \frac{\delta \otimes_{r,\max}}{2\sqrt{3}} \quad (16)$$

and likewise,

$$u(t_R) = \frac{\delta \otimes_{R,\max}}{2\sqrt{3}} \quad (17)$$

$\delta \otimes_i$ The roundness deviation on the height of point I

The combined standard uncertainty $u(t)$ can be computed by taking the square root of the sum of squares of $u(t_r)$ and $u(t_R)$:

$$u(t) = \sqrt{u(t_r)^2 + u(t_R)^2} \quad (18)$$

3.4.3 Diameter measurements

The uncertainty due to the diameter measurements of the piston and cylinder are respectively represented by $u(d_r)$ and $u(d_R)$. During the length measurements process of the diameters of the PCC different elements, like for example the expansion coefficient of the PCC, influence the measurement and its result has to be corrected accordingly. For more information about the measurement process of NMI see Appendix A. To obtain the radius values of the PCC, the diameter is divided by two. The mathematical model [10] for the length measurement is:

$$\delta_d = l_i + \lambda + t \cdot e \cdot l_i + \Delta l_p + \Delta l_m + \delta l_a + \delta l_{dp} \quad \text{where } i = 1, \dots, n \quad (19)$$

δ_d diameter measurement after corrections

l_i laser reading in + and – direction

λ correction for laser wavelength

t temperature of the piston and cylinder

e expansion coefficient

Δl_p correction for the probe constant

Δl_m correction for the levelness of the mirror

δl_a alignment of the piston and cylinder

δl_{dp} dead path error

The combined standard uncertainty $u(d)$ can be computed by taking the square root of the sum of squares of $u(d_r)$ and $u(d_R)$:

$$u(d) = \sqrt{u(d_r)^2 + u(d_R)^2} \quad (20)$$

3.4.4 Uncertainty of the effective area computation

The total uncertainty is computed by multiplying the combined standard uncertainty with the coverage factor k . The coverage factor is usually set on two. When $k = 2$ the coverage probability for a Normal distribution is approximately 95%.

First the combined standard uncertainty of the three before mentioned components need to be computed by multiplying the square root of the sum of squares of $u(s)$, $u(t)$ and $u(d)$ by the partial derivative of equation (10).

To determine the total uncertainty of the effective area the combined standard uncertainty has to be multiplied by the coverage factor k .

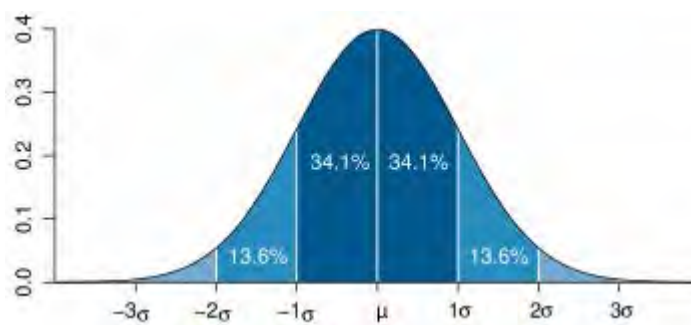


Figure 3.3 The Coverage factor

The value of the coverage factor is based on the desired level of confidence to be associated with the interval defined by $u(y) = c_i u(x_i)$. When the normal distribution applies $k = 2$ defines an interval with a level of confidence of approximately 95 %, and $k = 3$ defines an interval with level of confidence of approximately 99 % (see Figure 3.3).

The derivative of the function $f = \pi(r^*)^2$ that is used to calculate the effective area is $f' = 2 \pi r^*$

$$u^2(A_0) = k f' \sqrt{u(s)^2 + u(s)^2 + u(d)^2} \quad (21)$$

k	Coverage factor
$u(s)$	Uncertainty due to the shape deviation of the PCC
$u(t)$	Uncertainty due to the roundness deviation of the PCC
$u(l)$	Uncertainty due to the error in the length measurement of the PCC

3.5 Application on NMI dataset

In this section the effective area and the corresponding uncertainty will be computed. The dataset of the NMI that can be seen in Table 3.1 will be used.

3.5.1 Effective area calculation

$$\bar{r} = 17.6663 \text{ mm}$$

$$\bar{R} = 17.6673 \text{ mm}$$

$$r^* = \frac{\bar{r} + \bar{R}}{2} = 17.6668$$

$$A_{eff} = \pi \cdot (r^*)^2 = \pi \cdot 17.6668^2 = 980.5434 \text{ mm}^2$$

The effective area of the DH350 PCC of the NMI is 980.5434 mm^2

3.5.2 Uncertainty calculation

The uncertainty of the effective area consists of three components: straightness, roundness and length measurements.

Straightness:

$$\sigma_r = 0.000014$$

$$\sigma_R = 0.00034$$

The NMI-DH350 dataset contains 15 points ($n = 15$). The standard uncertainties $u(s_r)$ and $u(s_R)$ will therefore become:

$$u(s_r) = \frac{0.000014}{\sqrt{15}} = 0.000004$$

$$u(s_R) = \frac{0.00034}{\sqrt{15}} = 0.00009$$

The combined standard uncertainty $u(s)$ is computed by,

$$u(s) = \sqrt{0.000004^2 + 0.00009^2} = 0.0000902.$$

Roundness

In Table 3.2 can be seen that the maximal roundness deviation of the piston ($\delta \otimes_{r,\max}$) is 0,000151 mm and of the cylinder ($\delta \otimes_{R,\max}$) is 0,000068 mm. The standard uncertainties $u(t_r)$ and $u(t_R)$ will therefore become:

$$u(t_r) = \frac{0.000151}{2\sqrt{3}} = 0.000043$$

$$u(t_R) = \frac{0.000068}{2\sqrt{3}} = 0.000019$$

The combined standard uncertainty $u(t)$ can then be computed by,

$$u(t) = \sqrt{0.000043^2 + 0.000019^2} = 0.000048.$$

Length measurements

The combined standard uncertainty $u(d)$ can be computed by taking the square root of the sum of squares of $u(d_r)$ and $u(d_R)$, where $u(d_r)$ (50 nm) and $u(d_R)$ (75 nm) are given by the Length Department of NMI.

$$u(d) = \sqrt{0.000050^2 + 0.000075^2} = 0.00009$$

Uncertainty of the effective area

$$u^2(A_0) = k f' \sqrt{u(s)^2 + u(s)^2 + u(d)^2}$$

The derivative of the function $\pi(r^*)^2$ that is used to calculate the effective area is:

$$f' = 2\pi r^*$$

With $r^* = 17.6668$ f' will become: 111.0039.

The coverage factor is usually set to two: $k = 2$

Filling this in the equation above:

$$u^2(A_0) = 2 \times 11.0039 \sqrt{0.00009^2 + 0.000048^2 + 0.00009^2} = 0.0305$$

Thus the effective area of NMI-DH350 is $980.5434 \pm 0.0305 \text{ mm}^2$.

Chapter 4 Dadson's theory

4.1 Introduction

In the previous chapter the model used by NMI to calculate the effective area of a PCC was discussed. Through the EUROMET project 740 the NMI was introduced to new models based on a theory described in "The Pressure Balance, Theory and Practice." [3]. For convenience we will refer to this method as Dadson's theory. Four (out of six) NMIs that participated in the before mentioned project have based their models on Dadson's theory and their results had a considerably lower uncertainty. Reason enough to discuss the theory in this chapter. Dadson starts with determining the effective area of an ideal PCC and slowly expands to a more complex model that calculates the effective area for a simple PCC.

4.2 The effective area of an ideal PCC

An ideal PCC is a PCC where the piston and cylinder have perfectly straight and straight cylindrical surfaces. The assumptions made in this model correspond to the ones made for the model used by the NMI, namely:

1. The midpoint is the same on every height
2. They share the same midpoint.
3. They are perfectly round at every height.
4. They are perfectly straight at every height.

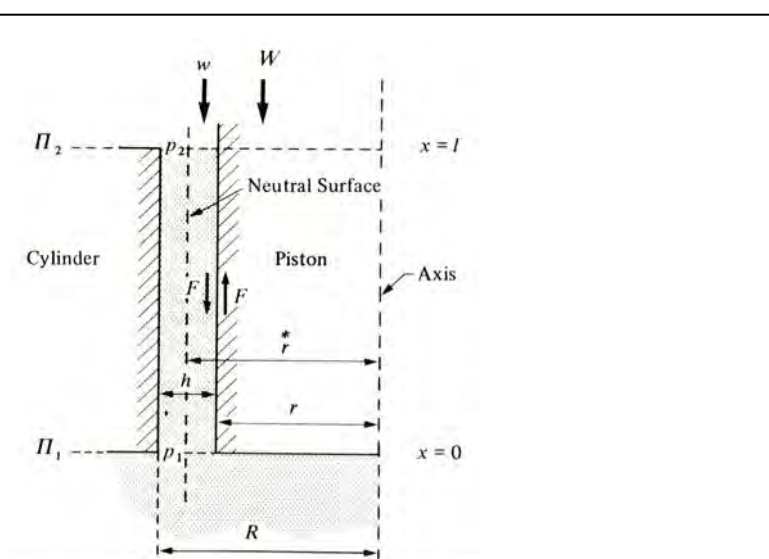


Figure 4.1: Schematic diagram of a PCC [3]

An schematic representation of the ideal PCC is shown in Figure 4.1. The fluid pressure p_1 is measured at the bottom of the piston at the level $x = 0$, while the top of the piston (level $x = l$) will be exposed to the ambient pressure p_2 . The measurement process consists of balancing the upward force arising from the difference between the two pressures ($p_1 - p_2$) against a downward gravitational force which is applied to the piston by a group of calibrated masses including that of the piston itself. The radii of the piston, cylinder and effective area are given respectively by r , R and r^* .

4.2.1 The virtual piston model

The upward force on the piston has besides the pressure difference also an frictional part F . Because of the pressure difference the fluid in the PCC is forced to move upwards and thereby exerts pressure on the flanks of the piston. Let W' denote the true value of the corrected downward gravitational force due to the applied masses including that of the piston. Then W' can be determined by equilibrating the forces acting on the piston by the equation:

$$W' = \pi r^2 (p_1 - p_2) + F \quad (22)$$

- W' = Downward gravitational force on W
- r = Radius of the piston
- F = Frictional force
- $p_1 - p_2$ = Pressure difference

The cylindrical surface of radius r^* is often termed the 'neutral surface' [3] which is the same as the effective area and is shown by the broken line in Figure 4.1. In the case of plane-parallel surfaces the neutral surface would be a plane situated precisely midway between the two boundaries, which is assumed by NMI.

The weight of the ring shaped cross-section that is contained between the surfaces of the piston and the neutral surface is referred to by w and the downward gravitational force due to its mass is denoted by w' . When you include the force F that is exerted on the flanks of the piston by the fluid that is pressed upwards, the following equation is obtained:

$$w' + F = \pi (r^{*2} - r^2) (p_1 - p_2) \quad (23)$$

- w' = Downward gravitational force on w
- r^* = Radius of the neutral surface

Equation (22) and (23) combined give

$$W' + w' = \pi r^{*2} (p_1 - p_2), \quad (24)$$

which can be reduced to the form $W = A p$. The effective area A_{eff} of the assembly is therefore given very simply by

$$A_{eff} = \frac{W' + w'}{p_1 - p_2} = \pi r^{*2} , \quad (25)$$

so the effective area is equal to the cross-sectional area of the PCC whose boundary is the neutral surface. This causes the load on the piston to increase due to the mass of the ring shaped column of fluid between this surface and that of the piston (w'). In other words, the actual piston could be replaced by a ‘virtual piston’, which surface is determined by the radius of the neutral surface. That is why it is called the virtual piston model.

4.2.2 Location of the neutral surface

The real question is what the value of r^* should be. In the last paragraph it was mentioned that with the small gap in the PCC it is usually a close enough approximation to treat the neutral surface as if it is lying halfway in between the piston and cylinder (plane-parallel surfaces). However, it turns out that slightly differing approximations have been used in literature, and therefore this is further examined in [3].

It is shown that the exact result follows from the classical theory of viscous flow between cylindrical surfaces, where it may be shown that:

$$r^* = \frac{(R^2 - r^2)}{2 \ln\left(\frac{R}{r}\right)}. \quad (26)$$

Since the fields R and r are approximately equal the following equation is obtained [3]

$$R = r(1 + \varepsilon) \quad (27)$$

with $\varepsilon = \frac{R}{r} - 1$

Here ε is a very small number and terms ε^3 may be neglected. If the logarithmic term is expanded to the second order in ε , we find

$$r^* = r^2 \left(1 + \varepsilon + \frac{\varepsilon^2}{6} \right). \quad (28)$$

In the case of pressure-balance assemblies ε is not likely to be greater than 10^{-3} , i.e. ε^2 is not likely to be greater than 10^{-6} , and will often be much less. Later in [3] the third form of approximation $r^* = r^2(1 + \varepsilon)$ has been used with the main concern of avoiding the unnecessary complication in the further on mentioned formulas for effective areas. Equation (25) can then be reduced to

$$S = \pi r^2 \left(1 + \frac{h}{r} \right), \quad (29)$$

where h is the radial clearance ($R - r$) between the two surfaces. The crucial assumption here is that both R and r have small variations and that their difference h is small compared to the radii.

4.3 The effective area for a simple PCC

The next step is to extend the virtual piston model given above by considering assemblies in which the radii of the piston and cylinder may vary on different heights but in which there is still circular symmetry.

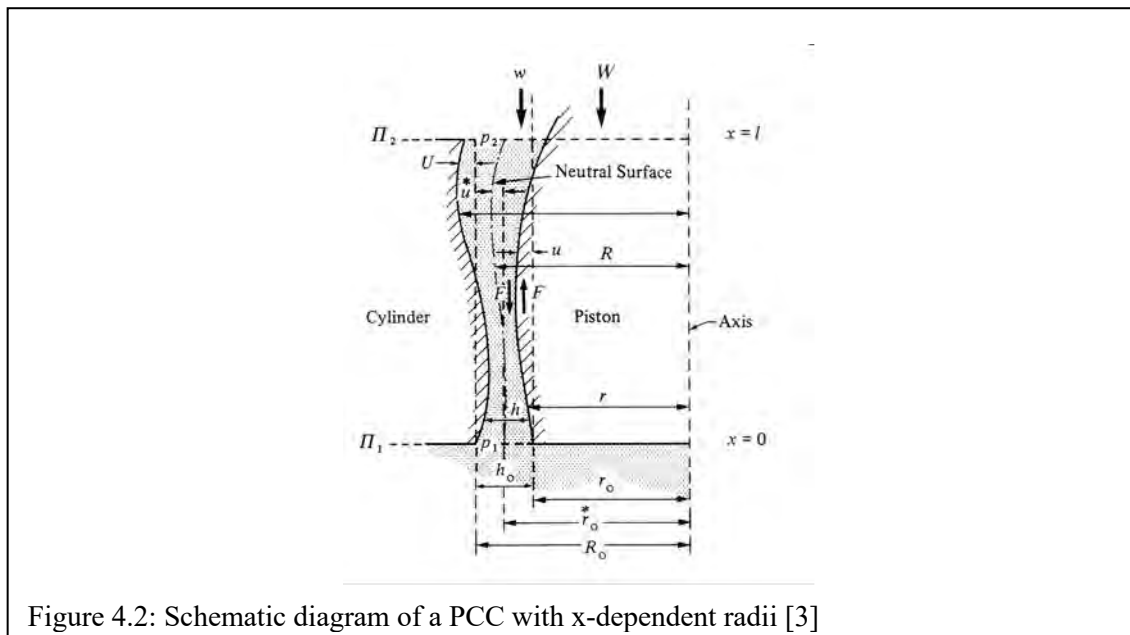


Figure 4.2: Schematic diagram of a PCC with x-dependent radii [3]

A cross-section of this model can be seen in Figure 4.2, where u and U stands for deviations in r and R , using 0 for values of the dimensions at the reference level $x = 0$. The upward force on the piston is built up from [3]:

1. a force equal to $\pi r_0^2 p_1 - \pi (r_0 + u_2)^2 p_2$ due to the actual pressures acting on the ends of the piston;
2. a frictional force F , exerted on the flanks of the piston by the fluid which is being forced to move upwards under the influence of the pressure gradient;
3. a force equal to $2\pi \int_0^l r(p - p_2) \frac{du}{dx} dx$ due to the vertical component of the fluid pressure acting on those parts of the flanks of the piston which are inclined to the vertical axis.

Equation (22) now becomes, after some reduction

$$W' = \pi r_0^2 (p_1 - p_2) + 2\pi \int_0^l r (p - p_2) \frac{du}{dx} dx + F \quad (30)$$

If you compare equation (30) with (22) of the virtual piston model, it can be seen that (28) considers the extra frictional component described by 3.

Balancing the forces acting on the ring shaped column of fluid between the surface of the piston and the neutral surface, equation (24) becomes,

$$w' + F + 2\pi \int_0^l r (p - p_2) \frac{du}{dx} dx = \pi (r_0^{*2} - r_0^2) (p_1 - p_2) + 2\pi \int_0^l r^* (p - p_2) \frac{du^*}{dx} dx \quad (31)$$

By the addition of equation (24) and (25) equation (32) is obtained:

$$W' + w' = \pi r_0^{*2} (p_1 - p_2) + 2\pi \int_0^l r^* (p - p_2) \frac{du^*}{dx} dx. \quad (32)$$

Where $2\pi \int_0^l r^* (p - p_2) \frac{du^*}{dx} dx$ is a force equal to the vertical component of the fluid pressure.

If you divide both parts of equation (32) by $(p_1 - p_2)$ the expression for the effective area, corresponding to equation (25), will become

$$A_{eff} = \frac{W' + w'}{p_1 - p_2} = \pi r_0^{*2} + \frac{2\pi}{(p_1 - p_2)} \int_0^l r^* (p - p_2) \frac{du^*}{dx} dx \quad (33)$$

In most cases it would be unnecessary to include terms of the second order in ε , and therefore the expression can be reduce to

$$A_{eff} = \pi r_0^2 \left\{ 1 + \frac{h_0}{r_0} + \frac{1}{r_0 (p_1 - p_2)} \int_0^l (p - p_2) \frac{d(u + U)}{dx} dx \right\} \quad (34)$$

which is the generalization of equation (29).

Now the distribution of the pressure p as a function of x has to be determined, which will depend on the distribution of the radial deviation u and U . Next to the radial deviations the main parameters, density and viscosity of the fluid in the small space between the piston and cylinder, are expressed as functions of the pressure. In the case of PCCs that use incompressible fluids, [3] regards that the density and viscosity of a pressure transmitting liquid as oil is independent of pressure. Equation (34) then becomes:

$$A_{eff} = \pi r_0^2 \left\{ 1 + \frac{h_0}{r_0} + \frac{1}{r_0} \frac{\int_0^l \frac{(u + U)}{h^3} dx}{\int_0^l \frac{1}{h^3} dx} \right\} \quad (35)$$

However we will not go deeper into this matter and for further information on this subject the reader is referred to '*The Pressure Balance, Theory and Practice*'. For PCCs that use compressible fluids and where the applied pressure tends to zero the expression for effective area is identical to (35).

Chapter 5 Proposed model

5.1 Introduction

In the last two chapters, two models were discussed: the model based on Dadson's theory and the model used by NMI. The main difference between both models is that NMI's model, ignores the extra friction component F discussed in chapter 4, in contrast to the model based on Dadson's theory. In this chapter a new model is proposed. In the next section we will discuss why the "straight assumption" should be dropped.

5.2 Perfectly straight or not?

In modelling, assumptions have to be made to reduce a problem so that it is possible to have it modelled given the data available. The challenge is to find a model that describes reality as accurate as possible, again given the data available.

The main difference between the NMI model and the model based on Dadson's theory is that Dadson does not assume that the piston and cylinder are perfectly straight, which means that they do not assume that the radius is the same on every height. In Dadson's model this results in the piston and cylinder radii being dependent of an index that represents the height of the measured point and thereby reckons the imperfections in the PCC. In the NMI model, two radii are calculated for characterising the piston and cylinder respectively.

Another effect from leaving the straightness assumption out is the acknowledgement of the frictional force F . This force is a result of the friction that is caused by the movement of the fluid in the small gap between the piston and cylinder. So if the NMI would drop this assumption, it would make their model more credible.

Now that the perfectly straight assumption is dropped a new model is needed. As discussed in chapter four, the following equation is the basis of Dadson's model for effective area calculations [3]:

$$A_{eff} = \pi r_0^2 \left\{ 1 + \frac{h_0}{r_0} + \frac{1}{r_0} \frac{\int_0^l \frac{(u+U)}{h^3} dx}{\int_0^l \frac{1}{h^3} dx} \right\}, \quad (35)$$

where

- r_0 Radius of the piston at height $x = 0$
- R_0 Radius of the cylinder at height $x = 0$
- h_0 Radial clearance between R_0 and r_0
- u Difference between r_x and r_0 for $x = 1, .. n$
- U Difference between R_x and R_0 for $x = 1, .. n$
- h Radial clearance between R_x and r_x for $x = 1, .. n$

Equation (34) contains two integrals $\int_0^l \frac{(u+U)}{h^3} dx$ and $\int_0^l \frac{1}{h^3} dx$, where U , u and h are discrete series (see Table 5.1). A way to calculate these integrals is through the use of algorithms that can approximate integrals, like the trapezium rule, which will be discussed in the next section.

x	u	U	u + U	h
0	0.00000	0.00000	0.00000	0.00153
0.4	0.00000	-0.00004	-0.00004	0.00148
1.5	0.00000	-0.00006	-0.00006	0.00147
5.5	0.00002	-0.00066	-0.00064	0.00084
10.5	0.00000	-0.00084	-0.00084	0.00068
15.5	0.00000	-0.00090	-0.00090	0.00063
20.5	-0.00001	-0.00092	-0.00093	0.00061
25.5	-0.00002	-0.00089	-0.00091	0.00066
30.5	-0.00002	-0.00085	-0.00087	0.00069
35.5	-0.00003	-0.00075	-0.00078	0.00080
39	-0.00002	-0.00035	-0.00037	0.00119
39.6	-0.00002	-0.00043	-0.00045	0.00111
40	-0.00002	-0.00041	-0.00043	0.00113

Table 5.1 Series that are derived from the radius measurements r and R

In Table 5.1 the values for u , U and h are given on height x where all the values are given in millimetres.

5.3 The trapezium rule

The trapezium rule or trapezoid rule is one of a family of formulas for numerical integration called Newton-Cotes formulas and is a way to approximately calculate the definite integral [7]:

$$\int_a^b f(x) dx . \tag{36}$$

The trapezium rule works by approximating the region under the graph of the function $f(x)$ by a trapezium and calculating its area. It follows that

$$\int_a^b f(x)dx \approx (b-a) \frac{f(a)+f(b)}{2}. \quad (37)$$

To calculate this integral more accurately, one first splits the interval of integration [a,b] into n smaller subintervals, and then applies the trapezium rule on each of them. One then obtains the composite trapezium rule:

$$\int_a^b f(x)dx \approx \frac{(b-a)}{2n} (f(x_0) + 2f(x_1) + 2f(x_2) + \dots + 2f(x_{n-1}) + f(x_n)). \quad (38)$$

where x_i denotes the radius measurement at level i with $i = 1, \dots, n$. The integration in equation (38) can be approximated by the following summation:

$$y = \frac{(b-a)}{n} \sum_{i=1}^{n-1} \frac{x_i + x_{i+1}}{2} = \frac{(b-a)}{n} \left(\frac{1}{2}x_1 + \sum_{i=2}^{n-1} x_i + \frac{1}{2}x_n \right), \quad (39)$$

which is of the form:

$$Y = \sum_{i=1}^n w_i X_i, \quad (40)$$

where X_i is a quantity that stands for the radius of the PCC and x_i is the i -th realization obtained through diameter measurements of the PCC. The trapezium rule is used to approximate the integrals $\int_0^l \frac{(u+U)}{h^3} dx$ and $\int_0^l \frac{1}{h^3} dx$.

Note that the Trapezium Rule can only be used on datasets where the distance between every x_i, x_{i+1} is the same. The new dataset of NMI (Table 5.3) meets this requirement.

5.4 Uncertainty

In the uncertainty model of the proposed model the straightness component has been dropped, because straightness is not assumed anymore. An uncertainty component that makes its entry is uncertainty due to the use of the Trapezium Rule, which will be discussed in section 5.4.1.

The uncertainty due to the length measurements is determined by the combined uncertainty of the diameter measurements and the roundness deviation (see sections 3.4.2 and 3.4.3):

$$u(l_r) = \sqrt{u(d_r)^2 + u(t_r)^2}$$

$$u(l_R) = \sqrt{u(d_R)^2 + u(t_R)^2}$$

The A_0 -uncertainty due to uncertainty of the length measurement is calculated by varying the piston and cylinder radii by their uncertainties. This method is more practical than determining

the partial derivative for every uncertainty component, because equation (35) is rather complex. In Table 5.2 the contributions to A_0 of the uncertainty due to the length measurements for the IMGC-100NNct PCC can be seen.

Variation	$\Delta A_0 / A_0$
$r^* = r + u(l_r)$	0.000010746
$r^* = r - u(l_r)$	-0.000010713
$R^* = R + u(l_R)$	0.000010133
$R^* = R - u(l_R)$	-0.000010101
Total effect	0.00002086

Table 5.2 Uncertainty contribution to A_0

The uncertainty due to the measurements of the piston $u(l_r)$ and cylinder $u(l_R)$ are both 26.3 nm. To calculate the total effect the sum of squares is calculated of the values in Table 5.2.

5.4.1 Uncertainties due to numerical procedures

Next is the determination of the uncertainty due to the use of the trapezium rule. Because it is assumed that the length measurement uncertainties are mutually independent we can use equation (42) to compute the uncertainty due to the use of the trapezium rule:

$$u^2(y) = \left(\frac{(b-a)}{n} \right)^2 \left(\frac{1}{4} u^2(x_1) + \sum_{i=2}^{n-1} u^2(x_i) + \frac{1}{4} u^2(x_n) \right) \quad (42)$$

For quadrature rules that can be written in the form of (40) and that are linear in the measured quantities X_i , the law of propagation of uncertainty based on a first-order Taylor series expansion can be applied, making no further approximation, to evaluate the uncertainty associated with the measurement result y . Such application gives:

$$u^2(y) = c^T V_x c, \quad (43)$$

where $c = (c_1, c_2, \dots, c_n)^T$ and V_x is the uncertainty matrix associated with the estimates x . In the case of mutually independent X_i , the result reduces to

$$u^2(y) = \sum_{i=1}^n c_i^2 u^2(x_i) \quad (44)$$

Equation (42) can be written in the form of (44) with weights,

$$c_i = \begin{cases} \left(\frac{(b-a)}{n} \right)^2 / 4, & i = 1, \\ \left(\frac{(b-a)}{n} \right)^2, & i = 2, \dots, n-1 \\ \left(\frac{(b-a)}{n} \right)^2 / 4, & i = n. \end{cases}$$

5.4.2 Systematic and random errors affecting the uncertainty

It is inconvenient that the obtained measurements r and R , which were used to calculate u , U and h , are not mutually independent. In the article “SWI Measure under pressure” [1] the following observation was made:

‘The piston diameter was measured at 13 different heights (ξ -coordinates), with a standard uncertainty of 50 nm, which is determined by the standard uncertainty of the measuring equipment. However, the sample standard deviation of these 13 measurements is only 14 nm.’

In cases where the data are assumed to be normally distributed the standard deviation is a good estimate for the uncertainty of a quantity. The quantity is a length measurement that has to be corrected for several influence factors, which are therefore also included in the uncertainty of the length measurement in model (19).

The length measurements are done with a laser and are denoted by l . In Table 5.3 the results of the laser readings on twenty different heights of a cylinder are shown. The minimum number of measurements at one height is three, but at four heights five measurements are taken. From these measurements the standard deviation is calculated. The standard deviations differ at every height. Apart from the first value all the standard deviations are smaller than 17 nm. To calculate the uncertainty of a radius measurement the standard deviation has to be divided by two. The other part of the uncertainty is determined by the influencing factors from the length measurement model.

These influencing factors are the same for every position. In the paper of SWI [1] it is concluded:

‘We conclude that the standard uncertainties of both piston and cylinder measurements must have a systematic and a random component. Both components are unknown, but the systematic component is always the same for all measurements, whereas the random components are independent from one another’.

x	Measurement number					σ	u(R)
	1	2	3	4	5		
38.1	35.33471	35.33475	35.33480	35.33478	35.33478	0.000035	17.2701
36.2	35.33435	35.33437	35.33437	35.33438	35.33438	0.000013	6.6885
34.3	35.33417	35.33417	35.33419	-	-	0.000016	7.8098
32.4	35.33406	35.33407	35.33405	-	-	0.000007	3.6079
30.5	35.33398	35.33402	35.33400	-	-	0.000017	8.5499
28.6	35.33394	35.33391	35.33395	-	-	0.000018	8.8857
26.7	35.33390	35.33391	35.33390	-	-	0.000009	4.3507
24.8	35.33385	35.33388	35.33386	-	-	0.000016	7.7697
22.9	35.33382	35.33382	35.33381	-	-	0.000003	1.5079
21	35.33379	35.33380	35.33380	-	-	0.000004	2.0230
19.1	35.33376	35.33378	35.33379	35.33377	35.33377	0.000009	4.3245
17.2	35.33378	35.33377	35.33378	-	-	0.000005	2.5119
15.3	35.33379	35.33379	35.33378	-	-	0.000008	4.0108
13.4	35.33382	35.33380	35.33381	-	-	0.000006	3.0439
11.5	35.33385	35.33388	35.33385	-	-	0.000017	8.6622
9.6	35.33387	35.33384	35.33386	-	-	0.000015	7.5432
7.7	35.33388	35.33391	35.33391	-	-	0.000015	7.3640
5.8	35.33400	35.33402	35.33402	-	-	0.000011	5.2884
3.9	35.33430	35.33429	35.33430	-	-	0.000007	3.6158
2	35.33471	35.33469	35.33471	35.33473	35.33472	0.000013	6.4901

Table 5.3 Length measurements of a cylinder in mm

The laser readings are assumed to be independent. One laser reading does not influence another one and its uncertainty can therefore be called random. The influence factors are the same for one measurement session and the uncertainty due to the influence factors can therefore be called systematic. Because the results of the measurements are not fully independent the propagation formula,

$$u^2(y) = \sum_i c_i^2 u^2(x_i) + \sum_{i=1}^{n-1} \sum_{j=i+1}^n c_i c_j u(x_i, x_j), \quad (45)$$

has to be used. Where c_i denotes the sensitivity coefficient. The sensitivity coefficient is the partial derivative of the measurement model f with respect to one of the input quantities x_i . It expresses the sensitivity of the uncertainty in y for the uncertainty in x_i .

The uncertainty propagation formula can be written in matrix form as follows [2]:

$$u^2(y) = \mathbf{c} V_x \mathbf{c}^T, \quad (46)$$

where \mathbf{c}^T denotes the transpose of the row vector \mathbf{c} and V_x denotes the uncertainty matrix of the input variables.

In Appendix B will be shown how the propagation rule can be applied to the length measurement uncertainty model of the NMI.

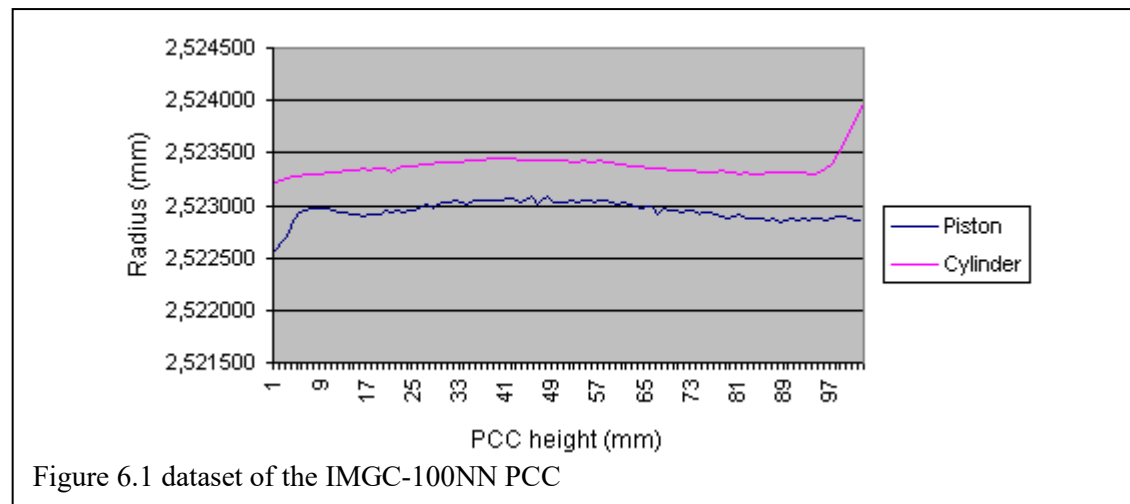
Chapter 6 Results

6.1 Introduction

In the previous chapters different models were discussed that led to the proposed model in chapter 5. To test the results of these models they were implemented in C. A short description of the different calculation methods of the effective area are given in the first paragraph. Finally we will compare these results with those of the PTB, the NMI of Germany, whose model is also based on Dadson's theory. The results of the PTB are almost similar to those of the SMU, LNE and IMGC.

6.2 Datasets

The input for the program consists of the height of the measurements, piston and cylinder radii and the difference between the latter two. The following datasets of six different PCCs were used: PTB-DH7594, IMGC-DH20L, IMGC-100NN, IMGC-DH500, NMI-DH350 and SMU-PG04. A graphical representation of the IMGC-100NN dataset can be seen in Figure 6.1.

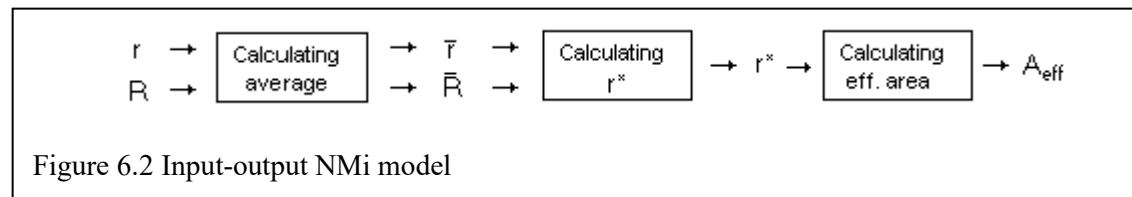


In Figure 6.1 it is clearly visible that at both the top of the cylinder and the bottom of the piston there is a matter of deformation, which is a common occurrence near the edge of an object.

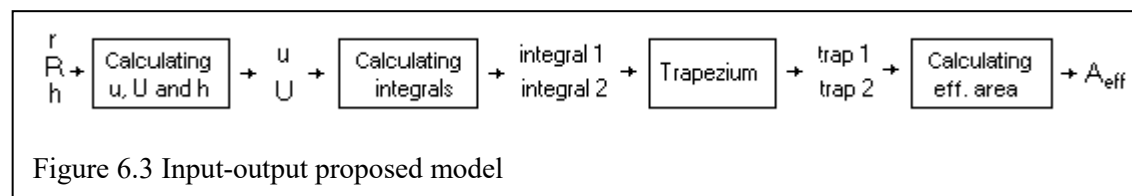
6.3 Effective area calculations

In Figure 6.2 you can see how the program determines the input and output of the NMI model. The diagram speaks for itself. First the input file, containing the dataset with values of r , R and

\mathbf{h} is read and their averages are computed. The next step is to determine the radius of the neutral surface r^* , which then is used to calculate the effective area.



In Figure 6.3 a diagram of the calculation process of the implemented proposed model can be seen. Equation (34) contains two integrals $\int_0^l \frac{(u+U)}{h^3} dx$ and $\int_0^l \frac{1}{h^3} dx$, where the variables U , u and h (see Table 4.1) are used.



When values of the input variables \mathbf{r} , \mathbf{R} and \mathbf{h} are read from the dataset, the first step in calculating the effective area is to compute the variables \mathbf{u} and \mathbf{U} . When \mathbf{u} , \mathbf{U} and \mathbf{h} are known the function values of the integrals have to be calculated, which results in two vectors: `integral1` and `integral2`. Through the use of the Trapezium rule (section 5.3) both integrals are computed and their value is saved in the variables `trap1` and `trap2`. In the last step `trap1` and `trap2` are filled in equation (34) and the effective area is calculated.

Dataset	PTB mm ²	Proposed mm ²	NMI mm ²
PTB-DH7594	4.90213920	4.90214000	4.90245400
IMGC-DH20L	49.02506600	49.02508000	49.02649000
IMGC-100NN	20.00056700	20.00057000	20.00049000
IMGC-DH500	1.96104360	1.96105200	1.96113700
Nmi-DH350	9.80527120	9.80530000	9.80543300
SMU-PG04	9.82330880	9.82338600	9.82321500

Table 6.1 Effective area values of three different methods

For six PCC's the effective area is calculated by the proposed model and the NMI model. The results of the program can be seen in Table 6.1. In [2], it was concluded that four out of six NMIs based their method on Dadson's theory. For that reason the results of these four NMIs were in line with each other. To verify the implementation of Dadson's theory, the results of the proposed and NMI model were compared with those of the PTB [9], the NMI of Germany. The

results seem not that different from each other, for that reason the difference between the two models and the PTB values will be compared in terms of percentage (Table 6.2).

Dataset	Proposed %	NMi %
PTB-DH7594	0.00002	0.00642
IMGC-DH20L	0.00003	0.00290
IMGC-100NN	0.00001	-0.00038
IMGC-DH500	0.00043	0.00476
NMi-DH350	0.00029	0.00165
SMU-PG04	0.00079	-0.00095

Table 6.2 Difference of both models to the PTB in terms of percentage

A better representation of the values in Table 6.2 can be seen in Figure 6.4. The values of the effective area calculations of the PTB are represented by the dark blue cubes on the zero-line. It is clearly visible that the values of the proposed model lie in line with the PTB values, in contrast to the results of the NMi model.

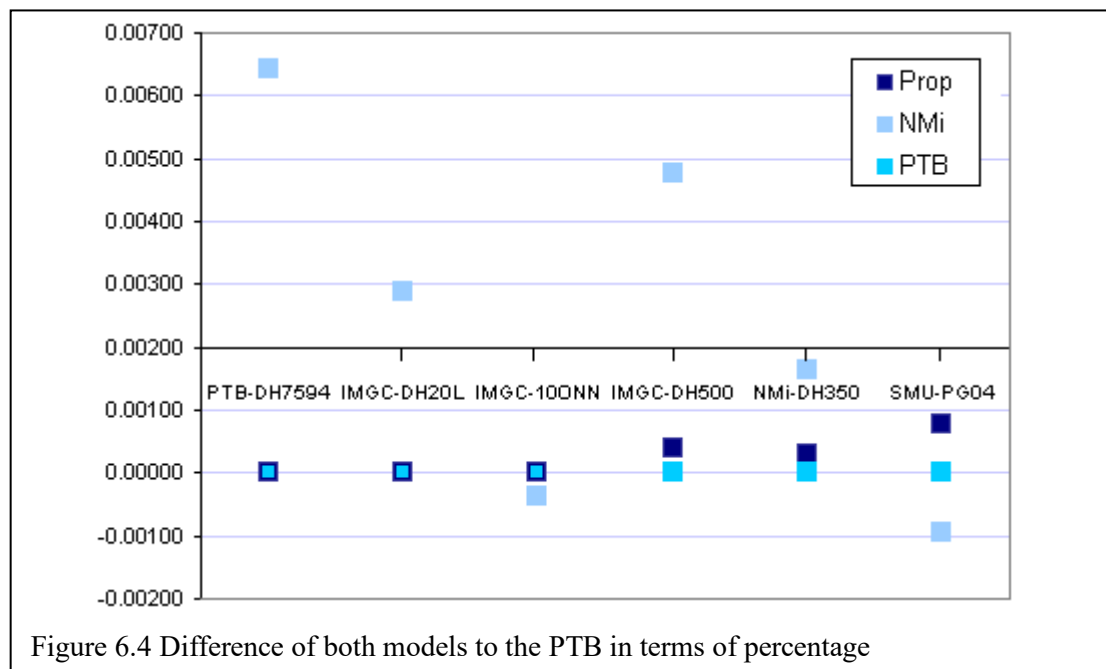


Figure 6.4 Difference of both models to the PTB in terms of percentage

Conclusion

The effective area of a PCC is the area on which the applied pressure is a function of the measurements and goniometry of both piston and cylinder. After the EUROMET Project 740 it became clear that NMI's approach to calculate the effective area leads to a different result and a higher uncertainty in comparison to the other participating institutions who based their models on Dadson's theory. The objective of this work has therefore been defined as:

'Studying Dadson's theory and the method used by the NMI to determine which method should be used to calculate the effective area in order to obtain a more accurate estimate and develop the corresponding uncertainty model'

In modeling assumptions have to be made to simplify a problem so that it is possible to have it modeled while it is still comprehensible and reliable. The main differences between the NMI model and the model based on Dadson's Theory is that Dadson does not assume that the piston and cylinder are perfectly straight. In Dadson's model this results in the piston and cylinder radii being dependent of an index that represents the height of the measured point and thereby reckons with the imperfections in the PCC.

As for the uncertainty of the effective area - due to the fact that the assumption that both piston and cylinder are perfectly straight is dropped, the corresponding uncertainty contribution is dropped as well. Another consequence of leaving the straightness assumption out is the acknowledgement of the extra frictional force F . This effect is included in the proposed model for the NMI.

Both models were implemented in C and their results were compared with the results of the PTB, the NMI of Germany, which are almost similar to those of the other participants of the EUROMET project. In contrast to the results of the NMI the results of the proposed model correspond to those of the PTB model which verifies the validity of the application of Dadson's theory in the proposed model. Therefore it can be concluded that the proposed model is more credible than the current NMI model, and that its results are in line with the results of the other participating NMI's.

Appendix

Appendix A NMI Measurement

The measurement of the piston or cylinder is performed with a coordinate measuring machine (CMM). First the probe constant is determined by measurements of an interferomic-calibrated end measure. Then the centre of the cylinder is determined and finally its diameter. The non-roundness is determined by two measurements with the help of roundness measuring machine and thereupon with the help of a software program the values are calculated.

The modeling of the cylinder measurement is revisited in order to determine the structure in the data. The radii at various heights have been reported with a standard uncertainty of 50 nm, whereas the standard deviation of the same radii is 14 nm, which makes it very unlikely that the data are independent [1]. In order to apply the law of propagation of uncertainty in as correct way, the correlations between the radii need be determined.

The objective of characterizing a piston is to determine its radius as a function of the height x . The characterization of a piston provides an estimate of the diameter (d), which is related to the radius as follows

$$r(x) = \frac{1}{2}d(x)$$

and hence

$$u(r) = \frac{1}{2}u(d)$$

If a series of n diameters is determined by

$$\mathbf{d} = \begin{bmatrix} d_1 \\ \dots \\ d_n \end{bmatrix}$$

then the relationship with the radii is given by

$$\mathbf{r} = \frac{1}{2}\mathbf{d}$$

The associated uncertainty matrix V_r can be computed from the uncertainty matrix associated with \mathbf{d} ,

$$V_r = \frac{1}{2}V_d$$

Furthermore, it is important to note that, apart from the uncertainty associated with the measurement of d_i , there is another component of uncertainty to be taken into account, namely the non-roundness. The model for the radius becomes

$$r_i = \frac{1}{2}(d_i + \delta d_{nr,i})$$

where the non-roundness is different at every height x (that is, for every index i). The value of δd_{nr} is zero for all i , and its associated uncertainty is determined from the roundness measurement.

The measurement of the radius R of the cylinder is performed in exactly the same way. The radius of the cylinder is given by

$$R_i = \frac{1}{2}(D_i + \delta D_{nr,i})$$

where D is the diameter measured by the CMM.

A.1 The measurement model for the diameter

The measurement of both the diameter of the cylinder and piston can be modeled as follows

$$d_i = l_i + \lambda + t \cdot e \cdot l_i + \Delta l_p + \Delta l_m + \delta l_a + \delta l_{dp} \quad (2)$$

- d_i reading of the diameter.
- l_i laser reading in + and – direction
- λ correction for laser wavelength
- t temperature of the piston and cylinder
- e expansion coefficient
- Δl_p correction for the probe constant
- Δl_m correction for the levelness of the mirror
- δl_a alignment of the piston and cylinder
- δl_{dp} dead path error
- i index of the measure level

The laser reading l_i can be expressed as $l_i = l_{+,i} - l_{-,i}$, where $l_{+,i}$ is the laser reading in the + direction and $l_{-,i}$ is the laser reading in the – direction. It is assumed that the readings are normally distributed. The laser readings in + and – direction are done 5 times. The result is defined as the average of the 5 readings

$$l_+ = \frac{1}{5} \sum l_{+(j)}$$

and

$$l_- = \frac{1}{5} \sum l_{-(j)}$$

Appendix B Uncertainty model

B.1 Uncertainty propagation

Many measurements are done indirectly, that is, several (input) quantities are measured and the quantity to be measured is subsequently calculated using a measurement model. Such a model is often explicit, that is, of the form

$$y = f(x_1, x_2, \dots, x_n).$$

If the uncertainty associated with the n input quantities x_i are known, the uncertainty associated with y can be expressed as follows using the uncertainty propagation formula,

$$u^2(y) = \sum_i c_i^2 u^2(x_i) + \sum_{i=1}^{n-1} \sum_{j=i+1}^n c_i c_j u(x_i, x_j) \quad (1)$$

Where c_i denotes the sensitivity coefficient. The sensitivity coefficient is the partial derivative of the measurement model f with respect to one of the input quantities x_i . It expresses the sensitivity of the uncertainty in y for the uncertainty in x_i .

The uncertainty propagation formula can be written in matrix form as follows []:

$$u^2(y) = \mathbf{c} V_x \mathbf{c}^T,$$

where \mathbf{c}^T denotes the transpose of the row vector \mathbf{c} and V_x denotes the uncertainty matrix of the input variables.

If the x_i are mutually independent and identically distributed, then the uncertainty matrix can be expressed as

$$V_x = u^2 I$$

where u denotes the standard uncertainty of one of the x_i and I the identity matrix. If the x_i are mutually independent, then the uncertainty matrix can be written as

$$V_x = \text{diag}\{u^2(x_1), u^2(x_2), \dots, u^2(x_n)\}$$

The matrix notation becomes in particular useful then the measurement model is of the form

$$y = F(\mathbf{x})$$

$$V_y = C V_x C^T$$

where on row i of C the sensitivity coefficients appear belonging to element y_i .

B.2 Example

Let the measurement model be

$$\Delta\lambda_i = x_i + y_i,$$

with index $i = 1, 2$ and uncertainty

$$u^2(\Delta\lambda_i) = u^2(x_i) + u^2(y_i).$$

Then the uncertainty matrix becomes

$$V_{\Delta\lambda} = C \cdot V \cdot C^T.$$

Output: $\Delta\lambda$
 Input: $(\mathbf{x}, \mathbf{y})^T$

Where $V = \begin{bmatrix} V_x & 0 \\ 0 & V_y \end{bmatrix}$ $C = \begin{bmatrix} \frac{\partial\Delta\lambda_1}{\partial x_1} & \frac{\partial\Delta\lambda_1}{\partial x_2} & \frac{\partial\Delta\lambda_1}{\partial y_1} & \frac{\partial\Delta\lambda_1}{\partial y_2} \\ \frac{\partial\Delta\lambda_2}{\partial x_1} & \frac{\partial\Delta\lambda_2}{\partial x_2} & \frac{\partial\Delta\lambda_2}{\partial y_1} & \frac{\partial\Delta\lambda_2}{\partial y_2} \\ \frac{\partial\Delta\lambda_3}{\partial x_1} & \frac{\partial\Delta\lambda_3}{\partial x_2} & \frac{\partial\Delta\lambda_3}{\partial y_1} & \frac{\partial\Delta\lambda_3}{\partial y_2} \end{bmatrix}$

$$C = \begin{bmatrix} 1 & 0 & 1 & 0 \\ 0 & 1 & 0 & 1 \end{bmatrix}$$

The variable x_i is determined by the variables a, b and z_i , and is composed as $x_i = a \cdot z_i + b$, where a and b are constants. The uncertainty matrix $V_x = C \cdot V \cdot C^T$.

Output: \mathbf{x}
 Input: $(a, b, \mathbf{z})^T$

Where $V = \begin{bmatrix} u^2(a) & 0 & 0 \\ 0 & u^2(b) & 0 \\ 0 & 0 & V_z \end{bmatrix}$ $C = \begin{bmatrix} \frac{\partial x_1}{\partial a} & \frac{\partial x_1}{\partial b} & \frac{\partial x_1}{\partial z_1} & \frac{\partial x_1}{\partial z_2} \\ \frac{\partial x_2}{\partial a} & \frac{\partial x_2}{\partial b} & \frac{\partial x_2}{\partial z_1} & \frac{\partial x_2}{\partial z_2} \\ \frac{\partial x_3}{\partial a} & \frac{\partial x_3}{\partial b} & \frac{\partial x_3}{\partial z_1} & \frac{\partial x_3}{\partial z_2} \end{bmatrix}$ $C = \begin{bmatrix} z_1 & 1 & a & 0 \\ z_2 & 1 & 0 & a \end{bmatrix}$

Where V_z is a 2 by 2 matrix with on the diagonal $u^2(z_1)$ and $u^2(z_2)$.

B.3 Propagation Model

Suppose that there are two diameter measurements, that is

$$\mathbf{d} = \begin{bmatrix} d_1 \\ d_2 \end{bmatrix}$$

The input variables follow from equation (1)

$$d_1 = l_1 + \lambda + t \cdot e \cdot l_1 + \Delta l_p + \Delta l_m + \delta l_a + \delta l_{dp} \quad (4)$$

$$d_2 = l_2 + \lambda + t \cdot e \cdot l_2 + \Delta l_p + \Delta l_m + \delta l_a + \delta l_{dp}$$

Let V be the uncertainty matrix associated with the vector $(l, \lambda, t, e, \Delta l_p, \Delta l_m, \delta l_a, \delta l_{dp})^T$ and the sensitivity matrix C the matrix that consists of sub matrices with the partial derivatives of the different variables.

Output: \mathbf{d}
 Input: $(l, \lambda, t, e, \Delta l_p, \Delta l_m, l_a, l_{dp})^T$

$$V = \begin{bmatrix} V_l & 0 & 0 & 0 & 0 & 0 & 0 & 0 \\ 0 & V_\lambda & 0 & 0 & 0 & 0 & 0 & 0 \\ 0 & 0 & V_t & 0 & 0 & 0 & 0 & 0 \\ 0 & 0 & 0 & V_e & 0 & 0 & 0 & 0 \\ 0 & 0 & 0 & 0 & V_p & 0 & 0 & 0 \\ 0 & 0 & 0 & 0 & 0 & V_m & 0 & 0 \\ 0 & 0 & 0 & 0 & 0 & 0 & V_a & 0 \\ 0 & 0 & 0 & 0 & 0 & 0 & 0 & V_{dp} \end{bmatrix}$$

$$C = \begin{bmatrix} \frac{\partial d_1}{\partial l_1} & \frac{\partial d_1}{\partial l_2} & \frac{\partial d_1}{\partial \lambda} & \frac{\partial d_1}{\partial t} & \frac{\partial d_1}{\partial e} & \frac{\partial d_1}{\partial \Delta l_p} & \frac{\partial d_1}{\partial \Delta l_m} & \frac{\partial d_1}{\partial l_a} & \frac{\partial d_1}{\partial l_{dp}} \\ \frac{\partial d_2}{\partial l_1} & \frac{\partial d_2}{\partial l_2} & \frac{\partial d_2}{\partial \lambda} & \frac{\partial d_2}{\partial t} & \frac{\partial d_2}{\partial e} & \frac{\partial d_2}{\partial \Delta l_p} & \frac{\partial d_2}{\partial \Delta l_m} & \frac{\partial d_2}{\partial l_a} & \frac{\partial d_2}{\partial l_{dp}} \end{bmatrix}$$

The variables $\lambda, \Delta x_p, \Delta x_m, l_a$ and l_{dp} are not related to any of the other variables and thereby have partial derivatives that are equal to the vector $\mathbf{1}$. The sensitivity matrix becomes:

$$C = \begin{bmatrix} 1 + T \cdot e & 0 & 1 & e \cdot l_1 & T \cdot l_1 & 1 & 1 & 1 & 1 \\ 0 & 1 + T \cdot e & 1 & e \cdot l_2 & T \cdot l_2 & 1 & 1 & 1 & 1 \end{bmatrix}$$

The uncertainty matrix of the **laser reading** is calculated as $V_l = CVC^T$ with input $\mathbf{l} = \begin{bmatrix} l_1 \\ l_2 \end{bmatrix}$.

$$\text{Where } V = \begin{bmatrix} u(l_1)^2 & 0 \\ 0 & u(l_2)^2 \end{bmatrix} \quad C = \begin{bmatrix} \frac{\partial l_1}{\partial l_1} & \frac{\partial l_1}{\partial l_2} \\ \frac{\partial l_2}{\partial l_1} & \frac{\partial l_2}{\partial l_2} \end{bmatrix} = [I_2]$$

The values of the parameters $\lambda, t, e, \Delta l_p, \Delta l_m, l_a$ and l_{dp} are on every level (i) the same and are thereby systematic. The uncertainty matrixes for these parameters are equal to their combined uncertainty that is constructed as $u^2(x) = c_x^2 u(x)^2$.

The uncertainty matrix of the **laser wavelength** V_λ is calculated as $V_\lambda = CVC^T$. With $\lambda = [\lambda_T \quad \lambda_p \quad \lambda_h \quad \lambda_{CO_2} \quad \lambda_E \quad \Delta\lambda]^T$ and the associated uncertainty matrix

$$V = \begin{bmatrix} u^2(\lambda_T) & 0 & 0 & 0 & 0 & 0 \\ 0 & u^2(\lambda_p) & 0 & 0 & 0 & 0 \\ 0 & 0 & u^2(\lambda_h) & 0 & 0 & 0 \\ 0 & 0 & 0 & u^2(\lambda_{CO_2}) & 0 & 0 \\ 0 & 0 & 0 & 0 & u^2(\lambda_E) & 0 \\ 0 & 0 & 0 & 0 & 0 & u^2(\Delta\lambda) \end{bmatrix}.$$

Then the expression for the sensitivity matrix associated with λ becomes

$$C = [c_1 \quad c_2 \quad c_3 \quad c_4 \quad c_5 \quad c_6]$$

The **laser wavelength** has a combined standard uncertainty of:

$$u^2(\lambda) = c_1^2 u^2(\lambda_T) + c_2^2 u^2(\lambda_p) + c_3^2 u^2(\lambda_h) + c_4^2 u^2(\lambda_{CO_2}) + c_5^2 u^2(\lambda_E) + c_6^2 u^2(\Delta\lambda)$$

The uncertainty matrix of the **alignment** is equal to $u^2(l_a)$. Where $l_a = a_x + a_l$, with a_x the alignment of the piston or cylinder and a_l the alignment of the laser. That leads to

$$u^2(l_a) = c_1^2 u(x_p)^2 + c_2^2 u(x_c)^2$$

Where $V = [u^2(l_a)]$ and $C = [c]$

The uncertainty matrices of the **temperature, expansion coefficient, probe constant and levelness of the mirror** are respectively $u^2(T) = c_T^2 u(T)^2$, $u^2(e) = c_e^2 u(e)^2$, $u^2(l_p) = c_p^2 u(l_p)^2$ and $u^2(l_m) = c_m^2 u(l_m)^2$.

The uncertainty associated with the **deadpath error** (l_{dp}) is a function of the ambient temperature, (Dp_T), pressure (Dp_p), humidity (Dp_h) and CO2 proportion (Dp_{CO_2}).

$$\begin{bmatrix} Dp_T \\ Dp_p \\ Dp_h \\ Dp_{CO_2} \end{bmatrix} \text{ and the associated uncertainty matrix } V_{x_{dp}} = CVC^T \text{ where}$$

$$V = \begin{bmatrix} V_T & 0 & 0 & 0 \\ 0 & V_p & 0 & 0 \\ 0 & 0 & V_h & 0 \\ 0 & 0 & 0 & V_{CO_2} \end{bmatrix}.$$

Then the expression for the sensitivity matrix C associated with Dp becomes

$$C = [c_1 \quad c_2 \quad c_3 \quad c_4]$$

$$u^2(\delta l_{dp}) = c_1^2 u(Dp_T)^2 + c_2^2 u(Dp_p)^2 + c_3^2 u(Dp_h)^2 + c_4^2 u(Dp_{CO_2})^2$$

So finally the uncertainty matrix V and the sensitivity matrix C become:

$$V = \begin{bmatrix} V_l & 0 & 0 & 0 & 0 & 0 & 0 & 0 \\ 0 & u^2(\lambda) & 0 & 0 & 0 & 0 & 0 & 0 \\ 0 & 0 & u^2(T) & 0 & 0 & 0 & 0 & 0 \\ 0 & 0 & 0 & u^2(e) & 0 & 0 & 0 & 0 \\ 0 & 0 & 0 & 0 & u^2(\delta l_a) & 0 & 0 & 0 \\ 0 & 0 & 0 & 0 & 0 & u^2(\delta l_p) & 0 & 0 \\ 0 & 0 & 0 & 0 & 0 & 0 & u^2(\delta l_{dp}) & 0 \\ 0 & 0 & 0 & 0 & 0 & 0 & 0 & u^2(\Delta l_m) \end{bmatrix}$$

$$C = \begin{bmatrix} 1+T \cdot e & 0 & 1 & e \cdot l_1 & T \cdot l_1 & 1 & 1 & 1 & 1 \\ 0 & 1+T \cdot e & 1 & e \cdot l_2 & T \cdot l_2 & 1 & 1 & 1 & 1 \end{bmatrix}$$

References

- [1] G. Molinar, M. Bergoglio, W. Sabuga, P. Otal, G. Ayyildiz, J. Verbeek, and P. Farar. Calculation of effective area A_0 for six piston-cylinder assemblies of pressure balances. Results of the EUROMET Project 740. *Metrologia*, 42:197–201, 2005.
- [2] M. Caubergh, J. Draisma, G. Franx, G. Hek, G. Prokert, S. Rienstra, A. Verhoeven. *Measure under Pressure: Calibration of pressure measurement*.
- [3] R.S. Dadson, S.L. Lewis, and G.N. Peggs. *The Pressure Balance: Theory and Practice*. HMSO, London, UK, 1982.
- [4] The Briannica Coincise Encyclopedia
- [5] BIPM, IEC, IFCC, ISO, IUPAC, IUPAP, OIML (1993) “Guide to the expression of uncertainty in measurement”, first edition, ISO Geneva, corrected print 1995
- [6] Theorie dictaat druk
- [7] J. Verbeek. NMI-DH350_rad with A_0 and U from NL corrected.xls, 2004
- [8] www.wikipedia.org
- [9] W. Sabuga. PTB results on EUROMET project 740: Effective area calculation, uncertainty evaluation and studies for piston-cylinder units of non-ideal geometries used in pressure balances (extended pressure range).
- [10] Length Department NMI, Onzekerheid ringen en pennen op CMM.xls, 2006.